Geophys. J. Int. (1991) **105**, 429–465

Traveltimes for global earthquake location and phase identification

B. L. N. Kennett[1] and E. R. Engdahl[2]
[1]*Research School of Earth Sciences, Australian National University, GPO Box 4, Canberra ACT 2601, Australia*
[2]*National Earthquake Information Center, US Geological Survey, Denver Federal Center, Box 25046, MS 967, Denver, CO 80225, USA*

Accepted 1990 December 3. Received 1990 November 24; in original form 1990 October 12

SUMMARY

Over the last three years, a major international effort has been made by the Sub-Commission on Earthquake Algorithms of the International Association of Seismology and the Physics of the Earth's Interior (IASPEI) to generate new global traveltime tables for seismic phases to update the tables of Jeffreys & Bullen (1940). The new tables are specifically designed for convenient computational use, with high-accuracy interpolation in both depth and range. The new *iasp91* traveltime tables are derived from a radially stratified velocity model which has been constructed so that the times for the major seismic phases are consistent with the reported times for events in the catalogue of the International Seismological Centre (ISC) for the period 1964–1987. The baseline for the *P*-wave traveltimes in the *iasp91* model has been adjusted to provide only a small bias in origin time for well-constrained events at the main nuclear testing sites around the world.

For *P*-waves at teleseismic distances, the new tables are about 0.7 s slower than the 1968 *P*-tables (Herrin 1968) and on average about 1.8–1.9 s faster than the Jeffreys & Bullen (1940) tables. For *S*-waves the teleseismic times lie between those of the JB tables and the results of Randall (1971).

Because the times for all phases are derived from the same velocity model, there is complete consistency between the traveltimes for different phases at different focal depths. The calculation scheme adopted for the new *iasp91* tables is that proposed by Buland & Chapman (1983). Tables of delay time as a function of slowness are stored for each traveltime branch, and interpolated using a specially designed tau spline which takes care of square-root singularities in the derivative of the traveltime curve at certain critical slownesses. With this representation, once the source depth is specified, it is straightforward to find the traveltime explicitly for a given epicentral distance. The computational cost is no higher than a conventional look-up table, but there is increased accuracy in constructing the traveltimes for a source at arbitrary depth. A further advantage over standard tables is that exactly the same procedure can be used for each phase. For a given source depth, it is therefore possible to generate very rapidly a comprehensive list of traveltimes and associated derivatives for the main seismic phases which could be observed at a given epicentral distance.

Key words: body waves, core phases, earthquake location, seismic phase identification, traveltimes.

INTRODUCTION

The standard traveltime tables used by seismological agencies such as the National Earthquake Information Center (NEIC) in Golden, Colorado, USA and the International Seismological Centre (ISC) in Newbury, UK are the Jeffreys & Bullen tables published in 1940. These tables were developed over the period 1930–1939 making use of reported arrival times of seismic phases at a sparse global network of stations, for which time keeping was frequently not reliable.

Although the limitations of these tables (Jeffreys & Bullen

1940), especially in the proper identification of later arriving core phases, have been recognized for some time, no other tables provide such a complete representation of the *P*, *S* and core phases. A major effort to improve *P*-wave traveltimes was made in 1968 based on the use of well-timed underground nuclear explosions as well as earthquakes (Herrin 1968). Subsequently a number of studies were made to try to improve knowledge of *S* times, either directly (Hales & Roberts 1970; Randall 1971) or via *S–P* differential times (Uhrhammer 1978).

The International Seismological Centre has built up a major database of the station readings used in establishing earthquake locations. This data set now extends over more than 20 years (1964–1988) with over 6 million arrival time readings at nearly 3000 seismic stations. This set of arrival times has been made available in digital form, originally on magnetic tape and recently for the period 1964–1987 on CD-ROM. Although the geographic distribution of stations is somewhat patchy and most sources occur in a limited number of seismic zones, the cumulative data set gives a good coverage of the interior of the Earth. The ISC data has played an important role in the development of recent earth models such as PREM (Dziewonski & Anderson 1981) and in studies of the lateral heterogeneity of the Earth (see e.g. Inoue *et al.* 1990).

With the extensive ISC data set, for a period where station time can be determined accurately, it is feasible to construct a set of traveltime tables for the major seismic phases with greater precision than Jeffreys & Bullen (1940) could attain. In 1987 the International Association of Seismology and the Physics of the Earth's Interior (IASPEI) requested its Subcommission on Earthquake Algorithms to propose a suitable set of traveltimes for use in global earthquake location. This paper describes the progress which has been made in the generation of such tables, and presents a set of summary tables for the main seismic phases. The primary form of the tables is a computational algorithm which is discussed in Appendix C.

THE REPRESENTATION OF SEISMIC TRAVELTIMES

The traditional approach to the construction of traveltime tables has been to develop smoothed, empirical representations of the traveltime curves for events of a certain depth. It was to this end that Jeffreys (1932, 1939) developed the 'method of uniform reduction' which was an important ingredient in the success of the work of Jeffreys & Bullen (1940). Once the traveltimes for the main phases have been constructed, the smoothed traveltime curves can be inverted using the Wiechert–Herglotz method to generate a velocity model. The times for ancillary phases can then be found by direct calculation from the velocity model.

The work of Jeffreys & Bullen was carried out entirely using hand-cranked calculators and, in consequence of the considerable labour involved, the traveltimes for the major phases are only tabulated for a limited number of depths. Interpolation in the Jeffreys & Bullen (1940) tables is therefore much more accurate in distance than in depth.

The major use of traveltime tables is in the location of earthquakes via computer algorithms, and so in constructing any new representation of the seismic traveltimes we must recognize that we should aim to optimize the ease of computational use. Summary printed tables provide a useful resource (especially for quick reference), but for seismogram interpretation it is highly desirable to have available a list of the characteristics of all the major phases at a given epicentral distance. Such information cannot readily be extracted from any current set of tables.

In order to achieve a consensus on an appropriate and practical representation for seismic traveltimes, the IASPEI Subcommission on Earthquake Algorithms held a workshop in October 1988 in Colorado, USA (Kennett 1988). This meeting brought together 15 participants from five countries with a wide range of expertise in earthquake location, traveltime calculation and studies of the Earth's interior.

After extensive discussion, general agreement was reached on the representation of the traveltimes by a radially stratified velocity structure to be constructed so that computed times would give as good a fit as possible to the teleseismic observations of *P*, *S* and core phases from the ISC catalogue. It should be stressed that such a velocity model is intended as a summary of seismic traveltimes and, because of the uneven geographic distribution of the ray paths sampled by the events in the ISC catalogue, will represent no simple average of the Earth. A major advantage of the use of traveltimes determined from an earth model is that the representation is consistent within and between different phases. In addition, for such a model, it is feasible to establish computationally effective means of both generating the traveltimes for selected phases for arbitrary source depth and range and also to display these in a form which is of considerable benefit to a seismic analyst.

In order to ensure that the specification of the traveltime tables is complete it is necessary to prescribe the interpolation procedure for the velocity model. There is also a need to provide a computationally efficient algorithm for access to the traveltime information for many phases for a given epicentral distance.

THE FORM OF THE VELOCITY MODEL

The agreed style of the velocity model employed to represent the traveltimes was the radial polynomial representation introduced in the PEM models (Dziewonski, Hales & Lapwood 1975). The model should be isotropic and the order of the interpolating polynomial chosen to be the same for both *P* and *S* wavespeeds, the discontinuities in *P* and *S* velocities should also be taken at the same depth. The crust and mantle structures would be chosen to be representative of continental regions because the vast majority of seismic stations lie on the continents.

The form of the model has been based on the PEM-C model (Dziewonski *et al.* 1975). The crust consists of two uniform layers with discontinuities at 20 and 35 km depth. In the upper mantle zone down to 760 km deep, the velocities in each layer are represented by a linear gradient in radius. The major mantle discontinuities were set at 410 and 660 km depth to give general agreement with the work of Revenaugh & Jordan (1989) on *S*-wave reverberations in the mantle. Other discontinuities were allowed at 120 and 210 km, and a discontinuity in velocity gradient at 760 km to give a smooth transition into the lower mantle. Such a

Table 1. Parametrized velocity model *iasp91*.

x = normalised radius r/a (a = 6371 km)

Depth z km	Radius r km	α km/s	β km/s
6371-5153.9	0-1217.1	11.24094 $-4.09689\,x^2$	3.56454 $-3.45241\,x^2$
5153.9-2889	1217.1-3482	10.03904 $3.75665\,x$ $-13.67046\,x^2$	0
2889-2740	3482-3631	14.49470 $-1.47089\,x$	8.16616 $-1.58206\,x$
2740-760	3631-5611	25.1486 $-41.1538\,x$ $+51.9932\,x^2$ $-26.6083\,x^3$	12.9303 $-21.2590\,x$ $+27.8988\,x^2$ $-14.1080\,x^3$
760-660	5611-5711	25.96984 $-16.93412\,x$	20.76890 $-16.53147\,x$
660-410	5711-5961	29.38896 $-21.40656\,x$	17.70732 $-13.50652\,x$
410-210	5961-6161	30.78765 $-23.25415\,x$	15.24213 $-11.08552\,x$
210-120	6161-6251	25.41389 $-17.69722\,x$	5.75020 $-1.27420\,x$
120-35	6251-6336	8.78541 $-0.74953\,x$	6.706231 $-2.248585\,x$
35-20	6336-6351	6.50	3.75
20-0	6351-6371	5.80	3.36

Table 2. P and S velocity values for model *iasp91* (100 km intervals).

depth km	radius km	α km/s	β km/s
6371.00	0.	11.2409	3.5645
6271.00	100.000	11.2399	3.5637
6171.00	200.000	11.2369	3.5611
6071.00	300.000	11.2319	3.5569
5971.00	400.000	11.2248	3.5509
5871.00	500.000	11.2157	3.5433
5771.00	600.000	11.2046	3.5339
5671.00	700.000	11.1915	3.5229
5571.00	800.000	11.1763	3.5101
5471.00	900.000	11.1592	3.4956
5371.00	1000.00	11.1400	3.4795
5271.00	1100.00	11.1188	3.4616
5171.00	1200.00	11.0956	3.4421
5153.90	1217.10	11.0914	3.4385
5153.90	1217.10	10.2578	0.
5071.00	1300.00	10.2364	0.
4971.00	1400.00	10.2044	0.
4871.00	1500.00	10.1657	0.
4771.00	1600.00	10.1203	0.
4671.00	1700.00	10.0681	0.
4571.00	1800.00	10.0092	0.
4471.00	1900.00	9.9435	0.
4371.00	2000.00	9.8711	0.
4271.00	2100.00	9.7920	0.
4171.00	2200.00	9.7062	0.
4071.00	2300.00	9.6136	0.
3971.00	2400.00	9.5142	0.
3871.00	2500.00	9.4082	0.
3771.00	2600.00	9.2954	0.
3671.00	2700.00	9.1758	0.
3571.00	2800.00	9.0496	0.
3471.00	2900.00	8.9166	0.
3371.00	3000.00	8.7768	0.
3271.00	3100.00	8.6303	0.
3171.00	3200.00	8.4771	0.
3071.00	3300.00	8.3171	0.
2971.00	3400.00	8.1504	0.
2889.00	3482.00	8.0087	0.
2889.00	3482.00	13.6908	7.3015
2871.00	3500.00	13.6866	7.2970
2771.00	3600.00	13.6636	7.2722
2740.00	3631.00	13.6564	7.2645
2740.00	3631.00	13.6564	7.2645
2671.00	3700.00	13.5725	7.2302
2571.00	3800.00	13.4531	7.1819
2471.00	3900.00	13.3359	7.1348
2371.00	4000.00	13.2203	7.0888
2271.00	4100.00	13.1055	7.0434
2171.00	4200.00	12.9911	6.9983
2071.00	4300.00	12.8764	6.9532
1971.00	4400.00	12.7607	6.9078
1871.00	4500.00	12.6435	6.8617
1771.00	4600.00	12.5241	6.8147
1671.00	4700.00	12.4020	6.7663
1571.00	4800.00	12.2764	6.7163
1471.00	4900.00	12.1469	6.6643
1371.00	5000.00	12.0127	6.6101
1271.00	5100.00	11.8732	6.5532
1171.00	5200.00	11.7279	6.4933
1071.00	5300.00	11.5761	6.4302
971.00	5400.00	11.4172	6.3635
871.00	5500.00	11.2506	6.2929
771.00	5600.00	11.0756	6.2180
760.00	5611.00	11.0558	6.2095
760.00	5611.00	11.0558	6.2095
671.00	5700.00	10.8192	5.9785
660.00	5711.00	10.7900	5.9500
660.00	5711.00	10.2000	5.6000
571.00	5800.00	9.9010	5.4113
471.00	5900.00	9.5650	5.1993
410.00	5961.00	9.3600	5.0700
410.00	5961.00	9.0300	4.8700
371.00	6000.00	8.8877	4.8021
271.00	6100.00	8.5227	4.6281
210.00	6161.00	8.3000	4.5220
210.00	6161.00	8.3000	4.5180
171.00	6200.00	8.1917	4.5102
120.00	6251.00	8.0500	4.5000
120.00	6251.00	8.0500	4.5000
71.00	6300.00	8.0442	4.4827
35.00	6336.00	8.0400	4.4700
35.00	6336.00	6.5000	3.7500
20.00	6351.00	6.5000	3.7500
20.00	6351.00	5.8000	3.3600
0.	6371.00	5.8000	3.3600

parametrization is adequate to represent the traveltimes for distances out to 30° even though it does not contain the level of complexity of models generated by matching observed and theoretical seismograms.

The wavespeed distribution in the lower mantle is represented by a cubic in radius between 760 and 2740 km. The velocities in the lowermost mantle are taken as a linear gradient in radius down to the core mantle boundary. In the core and inner core the velocity functions are specified as quadratic polynomials in radius.

The specific form of the velocity model which has been generated to represent the teleseismic traveltimes is shown in Tables 1, 2 and Fig. 1. The radii adopted for the inner core and outer core were guided by recent inversions for radial earth structure from high-accuracy free oscillation data (G. Masters, personal communication).

CALCULATION OF TRAVELTIMES

Traveltime tables designed for computer use need a compact but efficient form to minimize the computational cost of providing a specific piece of information. The currently used scheme in most global earthquake location procedures is to use a form of interpolation, in depth and range, in stored tables (Engdahl & Gunst 1966). This approach is very similar to the mode of working which would be adopted with the paper form of the Jeffreys & Bullen (1940) tables. Table interpolation requires a good deal of storage space since the traveltimes can be both discontinuous and multivalued as a function of range. In addition the epicentral distance spans for a traveltime branch for a single phase vary with hypocentral depth, and the flexibility of interpolation procedures ends up being limited by the special treatment required for each phase.

The present tables have been designed *ab initio* with computational implementation as the primary goal and so

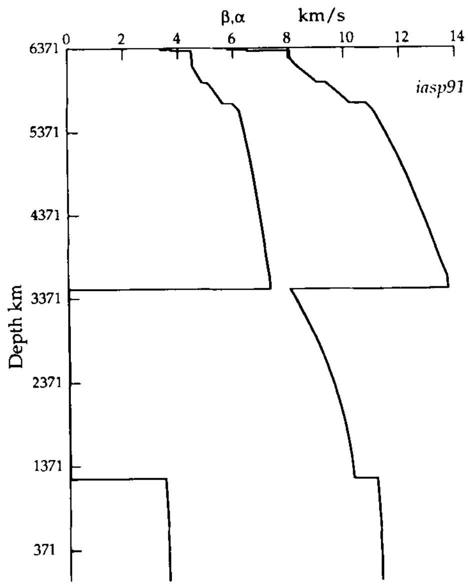

Figure 1. The *iasp91* velocity model.

we have adopted the tau-integral method of traveltime computation introduced by Buland & Chapman (1983). This procedure features a unified treatment for all types of seismic phases. For computational efficiency the form of calculation is table based but, instead of saving traveltimes, the delay times (tau) are tabulated as a function of source depth and ray parameter. In these tables the slownesses defining each branch are constant with depth and the tau function is monotonic and single-valued for each traveltime branch. Direct manipulation of the delay time tables yields traveltime as an explicit function of range without any need for an iteration on slowness. Interpolation in depth is also achieved to high accuracy by retaining delay-time contributions for portions of the model. For a source depth which is not already tabulated, the delay-time table as a function of slowness can be rapidly produced by combining the appropriate partial tau contributions with a pre-existing tau-table. This procedure means that we can readily compute the traveltimes for each phase at a particular source depth. In the summary tables we have therefore shown the times for each phase for a range of source depths rather than just the surface focus times with a depth correction table.

Further details of the traveltime computation technique are presented in Appendix C.

TEST EVENTS

The primary test of any proposed traveltime model is how well it performs in locating seismic events. The best measure of location errors is provided for events for which the location can be established by means other than by standard global location procedures. An effort has therefore been made to collect a set of events with a good geographic distribution across the globe and with well-constrained origin times and hypocentres. The events include explosions (mostly nuclear) and earthquakes which have been well located using local networks. A full list of the hypocentral parameters and magnitudes of the test events is presented in Appendix B.

A request for submission of test events was sent to a wide variety of seismolgoical observatories and agencies. The criteria for the selection of such events were as follows.

(a) For explosions

The events should be large enough to be recorded teleseismically ($m_b \geq 5$), and as far as possible the origin times, locations, and source depths should be known exactly.

(b) For earthquakes

The events should be impulsive simple sources well-recorded teleseismically. The origin times and hypocentres should be determined only with local network data and with a local structural model. Those local stations used should mostly be at near distances and reasonably well distributed in azimuth. If possible both *P* and *S* observations should be used. Unless the depth could be determined independently the local network data should include stations with direct *P* and *S* observations. The events should have origin times determined to better than 0.5 s and the absolute errors in the hypocentre should be less than 5 km. In order to enlarge the possible data set, some earthquakes with limited local network data, but with well-defined associated surface faulting, could also be included.

The initial response was somewhat slow but we have now built up a set of 83 earthquakes and 21 explosions with a reasonable distribution across the globe (see Figs 4 and 5). For each of these events, the use of local information should place stronger constraints on the depth of the event and the origin time than could be provided by teleseismic location alone. Although the majority of events are shallow, deeper focus events (>70 km) are represented from Alaska and Japan where dense local networks give close control. A full discussion of the test data set is provided by Engdahl & Buland (1991).

For each of the test events, as complete a set of traveltimes as possible was assembled using ISC data and additional phase contributions from contributors. The coverage for later phases is suprisingly good (see Fig. 6), and so it has proved possible to use the *P* readings to assess the performance of the new *iasp91* tables for location and the complete phase set as a check on the times of later phases.

THE CONSTRUCTION OF THE IASPEI 1991 TABLES

Following the 1988 workshop of the IASPEI Subcommision on Earthquake Algorithms, several of the participants worked on different aspects of the traveltime problem. E. R. Engdahl began the task of collecting well-controlled event parameters and associated phase data for the test events. K. Toy and A. M. Dziewonski (later with A. Morelli) undertook the selection of teleseismic data from the ISC catalogue and the inversion to generate suitable earth models. B. L. N. Kennett worked on the generation of an upper mantle model and later with R. Buland on the refinement of the software for traveltime calculation and table construction.

At the IASPEI General Assembly in Istanbul in August

1989, a further workshop was held at which progress towards the construction of the traveltime tables was reviewed. Two preliminary earth models *iasp89* [a composite model by Kennett using lower mantle velocities from Toy (1989a) and the core velocities from the PEM-C model] and *md89ps* (Morelli & Dziewonski 1989) were circulated in mid-1989. This allowed testing of the computational techniques and also comparison of the traveltimes with the observations for the available test events. Morelli & Dziewonski (1989) and Toy (1989b) presented different procedures for data selection from the vast ISC data catalogue, designed to maximize the geographic coverage of source–receiver paths and to optimize phase association especially for the later phases. The details of this work will be published elsewhere.

The velocity models derived by Morelli & Dziewonski (1989) and Toy (1989b), including allowance for event relocation, are very close in the lower mantle and the principal differences lie in the form of the upper mantle. Toy used a preliminary upper mantle model generated by Kennett which was characterized by rather large velocity jumps at the 410 and 660 km discontinuities. Morelli & Dziewonski favoured an upper mantle with smaller jumps but higher gradients.

For teleseismic P-waves the times predicted by the two models were in quite close agreement, and both were closer to the 1968 tables (Herrin 1968) than the Jeffreys & Bullen (1940) tables, reflecting a shift in baseline of approximately 2 s. For teleseismic S on the other hand, there was a noticeable offset between the times for the two models which hardly varied with distance.

Following the Istanbul workshop Kennett and Engdahl engaged in an iterative (and somewhat slowly converging) process to produce a final model. The form of the upper mantle velocity distribution was modified to represent a compromise between the styles of the *iasp89* and *md89ps* models and also to give a better fit to S times at shorter distances. Candidate velocity models were tested against an augmented set of test events and the influence of modifications in the velocity model were assessed.

Because the true origin time of earthquake sources are unknown there has always been some ambiguity in the absolute traveltimes which cannot be entirely eliminated by relocating events in the course of the inversion for velocity. A variation in the baseline for teleseismic traveltimes can be achieved with an adjustment of upper mantle velocities. A tilt of the traveltime distribution can be produced by maintaining the gradients in the lower mantle but varying the mean velocity in this zone.

The iterative development of the mantle velocity models was very revealing as to the nature of the hypocentral information provided for the test events and is discussed in more detail in Engdahl & Buland (1991). The final form of the velocity model *iasp91* (Tables 1, 2; Fig. 1) gives a very good fit indeed for the baseline provided by the subset of the test events consisting of nuclear explosions for which accurate origin times have been published (see Table 4).

REPRESENTATION OF TRAVELTIMES THROUGH THE UPPER MANTLE

An important ingredient in any representation of the traveltimes of seismic waves for the location of earthquakes is the set of times adopted to 30°. In this interval the seismic energy is returned from the crust, the uppermost mantle and the upper mantle transition zone. The velocity structures in these shallow zones are known to vary significantly with geographic location and so any 'average' description will inevitably be less effective than a regional model.

The approach followed by Jeffreys & Bullen (1940) was to build up the empirical traveltime tables by using data from those geographic regions where the source and station distribution provided sufficient data. Jeffreys (1970, section 3.101) gives a very clear account of the way in which the traveltimes for crustal and upper mantle paths were constructed.

The alternative procedure adopted for the 1968 P-tables (Herrin 1968) was to construct an artificial smooth model of the upper mantle whose times were representative of the central United States. As we have noted above, such a choice imposes a specific baseline on the teleseismic traveltimes.

Dziewonski & Anderson (1981, 1983) have derived summary traveltimes for surface focus at 1° intervals for both P- and S-waves from the ISC catalogues. In the 1983 study for P-waves these summary values include corrections for event relocation. The 1981 values for the S times did not allow for event relocation but with a 2 s baseline reduction the traveltime at 30° could be brought into close correspondence with the smoothed tables of Hales & Roberts (1970) and the tables of Gogna, Jeffreys & Shimshoni (1980) for central Asian earthquakes. These summary times are displayed in Table 3 and have been used to constrain the upper mantle portion of the model *iasp91*, together with the teleseismic residual bias and origin time errors for the test event data set.

The velocity model for the upper mantle down to 760 km

Table 3. Summary times to 30°.

Δ [°]	P [s]	S [s]
1.0	18.13	35.43
2.0	33.50	62.24
3.0	47.68	87.56
4.0	61.23	113.51
5.0	76.01	136.84
6.0	90.25	161.86
7.0	103.16	186.34
8.0	118.16	211.75
9.0	130.32	235.96
10.0	144.94	260.06
11.0	158.12	284.56
12.0	172.56	308.44
13.0	185.18	334.24
14.0	199.12	358.24
15.0	212.11	383.15
16.0	225.12	407.46
17.0	238.15	432.11
18.0	250.78	456.23
19.0	262.45	478.60
20.0	273.66	501.75
21.0	284.31	522.26
22.0	294.80	542.03
23.0	305.14	560.62
24.0	315.18	577.93
25.0	324.60	594.30
26.0	333.80	608.80
27.0	342.88	625.32
28.0	351.92	641.25
29.0	360.87	656.92
30.0	369.72	672.51

P values from Dziewonski & Anderson (1983)
S values from Dziewonski & Anderson (1981) reduced by 2 s baseline shift

was specified as constant layers in the crust and linear gradients in radius in the layers below. The traveltimes were therefore calculated using the analytic formulae due to Azbel & Yanovskaya (1972). The starting point for the construction of suitable velocity models was the PEM-C model of Dziewonski *et al.* (1975) with slight changes to the depths of discontinuities (*pemca* in Fig. 3). The summary traveltime data provide relatively weak constraints on the details of the velocity distribution and variety of styles of model give a similar level of fit to the data.

For *P*-waves, it was not necessary to introduce a low-velocity zone and at most a very weak discontinuity at 210 km could be sustained. The *iasp91* model gives a good match to the major changes in the slope of the traveltime curves (Fig. 2a).

For *S*-waves, it is less easy to fit the details of the summary traveltimes; this is likely to arise from difficulties in measuring *S* times and also considerable variability between regions. For example, Zielhuis (1988) reports up to 7 s difference between paths in southern Europe and the Baltic Shield using ISC data, as well as indications of offsets associated with low-velocity zones occurring over different distance ranges. The *iasp91* model gives a satisfactory fit to the *S*-wave summary times (Fig. 2b). The model does not include a low-velocity zone for *S* (even though this was included in the starting model *pemca*). The summary times show only weak direct evidence for a low-velocity zone (probably due to averaging over different structures). Although most *S* models for the upper model include a low-velocity zone, the *iasp91* model has the merit that there are no shadow zones for *S* for sources at any depth. As a result there are no holes in the traveltime curve.

The *iasp91* model has rather weak gradients down to 210 km and the computed times for *Sn* fit well with the summary times out to 18°. The general behaviour of the changes in the slope of the traveltime curve are also well matched. Around 22° the *PcP* traveltime curve cuts through the *S* branch and so there can be some difficulty with phase association in this interval.

The *iasp91* upper mantle model is plotted in Fig. 3 and compared with the starting model *pemca* and the isotropic version of PREM (Dziewonski & Anderson 1981) with a

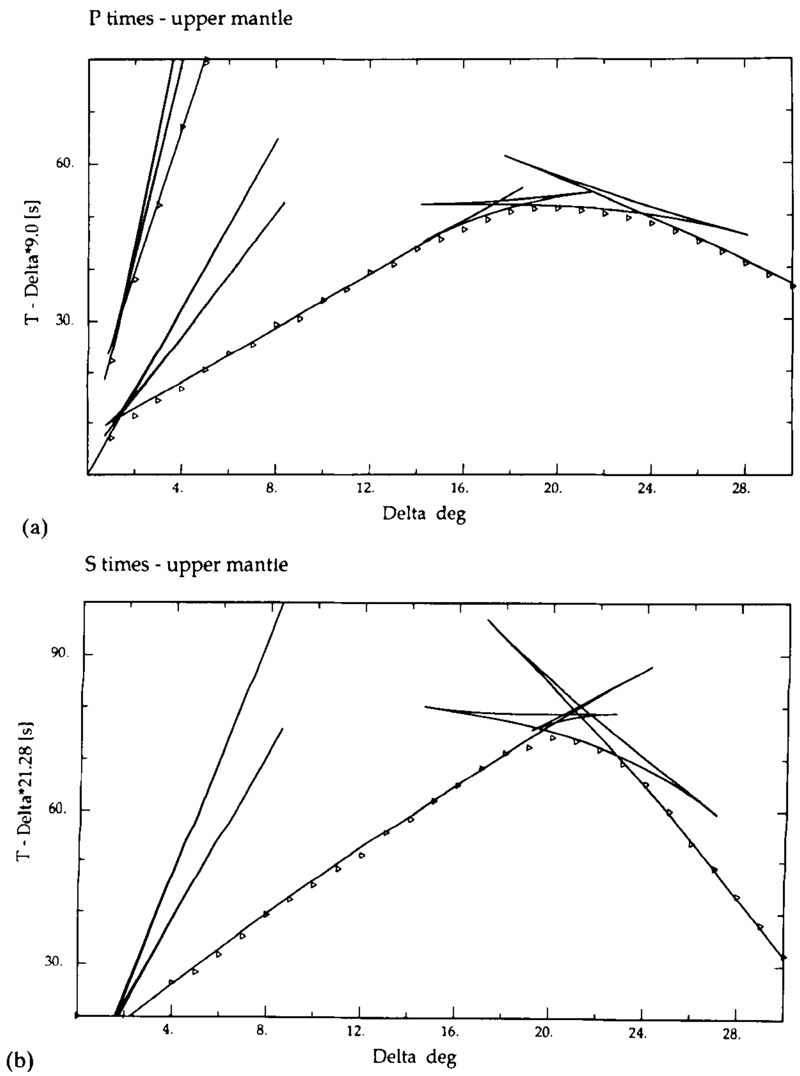

Figure 2. Upper mantle traveltime behaviour for model *iasp91* as a function of epicentral distance Δ: (a) fit to *P* summary times, (b) fit to *S* summary times.

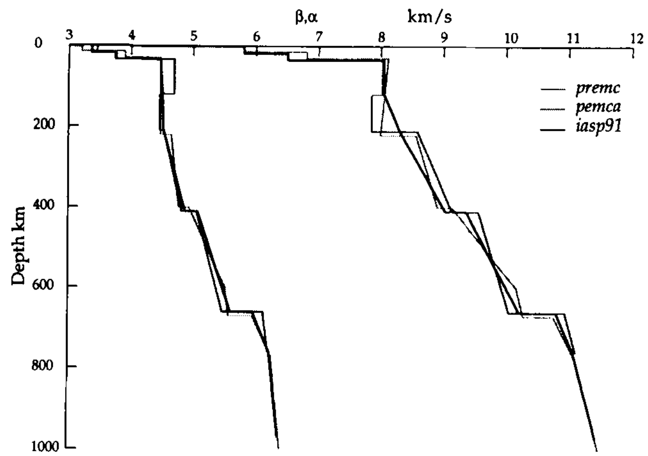

Figure 3. Comparison of *iasp91, pemca, premc* upper mantle velocity models.

superimposed continental crust (*premc*). The major differences are in the uppermost part of the models especially above the 210 km discontinuity; lateral heterogeneity is likely to be strongest in this zone. The *iasp91* model has been constructed for the specific purpose of representing the 'average' observed traveltimes for *P*- and *S*-waves out to 30° as well as providing a tie to teleseismic times. Since the distribution of seismic sources and seismic recording stations is far from uniform, we must expect that such a model will include geographical bias, in addition to the constraints provided by a specific parametrization.

For detailed studies in a particular region it would be appropriate to use a regional upper mantle model. The requirements for introducing regionalization are discussed in Appendix D.

LOWER MANTLE AND CORE STRUCTURE

Although the path coverage in the upper mantle is rather variable because of the disposition of seismic source and recording stations, it improves significantly for paths in the lower mantle. We may therefore expect that the velocity model for both *P*- and *S*-waves in the lower mantle will begin to approximate a spherical average.

P-waves

For *P*-waves, the principal constraint on mantle structure comes from the traveltimes of *P*-waves at teleseismic distances from 25° to 100°. Because *P* is a first arrival, it usually stands clear of the background noise for a reasonable size event, and so picking errors are not too large. For diffracted *P* beyond 95° the frequency and amplitude start to drop with range and the picking errors increase. The times for *P* for distances larger than 90° are not very sensitive to the details of the velocity near the core–mantle boundary. As a result the velocity gradient near the core–mantle boundary is not well constrained by traveltime data alone.

S-waves

For teleseismic *S*-waves the situation is less helpful. *S*-wave arrivals are lower frequency than *P* and have to be picked against the background of the *P*-wave coda. As a result, the picking error can be significant and is probably often of the order of 1 s.

In addition, the *S*-wave traveltime curve is cut by a number of other phases and so it may not always be easy to recognize *S*. For surface focus events there is a cross over with *ScP* near 40°, and of less significance with *PKiKP* near 60° and *SKiKP* near 75°. However, the major complications come from the intersection of the *S* and *SKS* traveltime branches near 80°. Because the *P*-wave velocity in the core is higher than the *S* velocity in the mantle, the *SKS*-wave with a significant core leg can overtake *S* at the same epicentral distance. The traveltimes of *S* and *SKS* are quite close (within 3 s) over the distance span from 81° to 86°. As a result phase association using time alone is very difficult in this distance range. Hales & Roberts (1970) endeavoured to resolve the difference by exploiting the polarization properties of *S* and *SKS* (there should be no *SH* component to *SKS* because it has undergone conversion to *P* in the core).

The path coverage of the lower mantle *S* velocity available from the teleseismic *S* traveltimes is therefore not complete. Nevertheless, the *S* velocity gradients can be well determined over most of the mantle via the cubic-polynomial representation of the velocity distribution. The *S* times for the velocity model *md89ps* (Morelli & Dzeiwonski 1989) are significantly offset from *iasp91*, but the offset is almost constant and arises from a different baseline associated with upper mantle structure. The shapes of the lower mantle distributions are quite similar.

CORE PHASES

For *P*-waves, the core is a low-velocity zone and this leads to the strong *PKP* caustic near 144°. The path to the A point is the shallowest sampled by any of the *PKP* branches and leaves a zone of nearly 800 km unsampled by *PKP* below the core–mantle boundary. *PKP* does give good coverage of the deeper core from the BC branches beyond 145° and of the outermost zone of the inner core from the DF branch which is most frequently reported between 110° and 125° and beyond 145°.

The shadow zone in the upper part of the core would be filled in with *PKKP* and higher core multiples of the type *PnKP* but reporting of these phases is somewhat patchy. A further source of information comes from *SKS* which does sample the outer core, but which adds in the effect of any uncertainties in the *S* velocity distribution in the mantle.

The core-phase traveltimes must currently be regarded as providing cross-checks on the results of inversions of free oscillations of the Earth for *P* velocity structure (as e.g. Dziewonski *et al.* 1975). The structure of the inner core cannot be well resolved by traveltimes alone. The jump in *P* velocity at the inner core boundary adopted for *iasp91* fits within the bounds derived by Cummins & Johnson (1989) from detailed amplitude studies.

MODEL TESTING

The construction of the *iasp91* velocity model has been based on the use of the ISC data base, but there is a long-recognized problem with possible errors in traveltimes.

These arise because, even after relocation of an event with a new velocity model, the origin times may well be in error. This error will propagate into the derived traveltimes. Also such errors may affect the procedure of phase association, which itself has to be based on a set of traveltimes. One measure of the error in absolute traveltime is the mean *teleseismic residual estimated* from the origin times and hypocentres provided by test event contributors.

The mean residual distribution in Fig. 4 shows general consistency in different regions. Some of the largest values are associated with earthquakes on oceanic islands (Hawaii, Iceland). Since the *iasp91* model has been constructed to have a continental crust, we would anticipate that there would be error introduced for shallow events in zones with rather different crustal and uppermost mantle structure. However, the errors are modest.

The patterns of the mean residuals reflect differences in the procedures used to generate the hypocentral information supplied for the test events. There is also a strong influence from the distribution of recording stations since the coverage of oceanic areas is limited.

We have mentioned above the difficulty of assigning a baseline from traveltime studies alone. Fortunately we have within the test events a subset of nuclear explosions for which independent information is available for the accurate origin time. The results for these well-calibrated events in the USA, USSR, Sahara and South Pacific are tabulated in Table 4. The mean teleseismic residual bias for the 14 events at the major test sites is 0.02 s, which is very encouraging indeed. If we include the five events away from the main test sites, the mean offset is still only 0.08 s. It would therefore appear that the baseline for the P times in the *iasp91* is in a satisfactory position.

The primary test of the *iasp91* tables is how well we are able to locate events where the hypocentral parameters are well constrained. We have therefore used the traveltimes for the *iasp91* model to estimate the hypocentral parameters of the 104 events (83 earthquakes, 21 explosions). Because the amount of regional data is somewhat variable between events, we have chosen to use only teleseimic times and to constrain the depth of all the test events at the values supplied with the event (which are tabulated in Appendix B). The location procedure then follows the standard NEIC practice but with the substitution of the *iasp91* tables for the Jeffreys & Bullen (1940) tables.

With a constrained depth solution, we have two convenient measures of the accuracy of the locations generated with the *iasp91* model; these are:

(a) the offset in origin time; and
(b) the mislocation vector for the epicentre.

The test events provide a reasonable geographic coverage of the globe as can be seen from Fig. 5, in which we display the mislocation vectors for the *iasp91* model. For those events where control on the origin time is strong, i.e. most of the explosions and a number of earthquakes, the origin time bias (see Table 4) is generally quite small (1 s or less) and there is tendency for the mean residual to be of similar magnitude but opposite sign.

Within the Nevada test site in the USA and the Soviet test site in Eastern Kazakhstan, there are systematic variations in the location performance which can be correlated with the position of the events within the test sites.

The influence of station distribution is also significant for the mislocation vectors and it is interesting to note that the distribution in Fig. 5 is quite similar to that for the JB times (and for other candidate models). The mean length of the mislocation vectors is not a strong function of the velocity model and the 13.8 km value for *iasp91* is almost the same

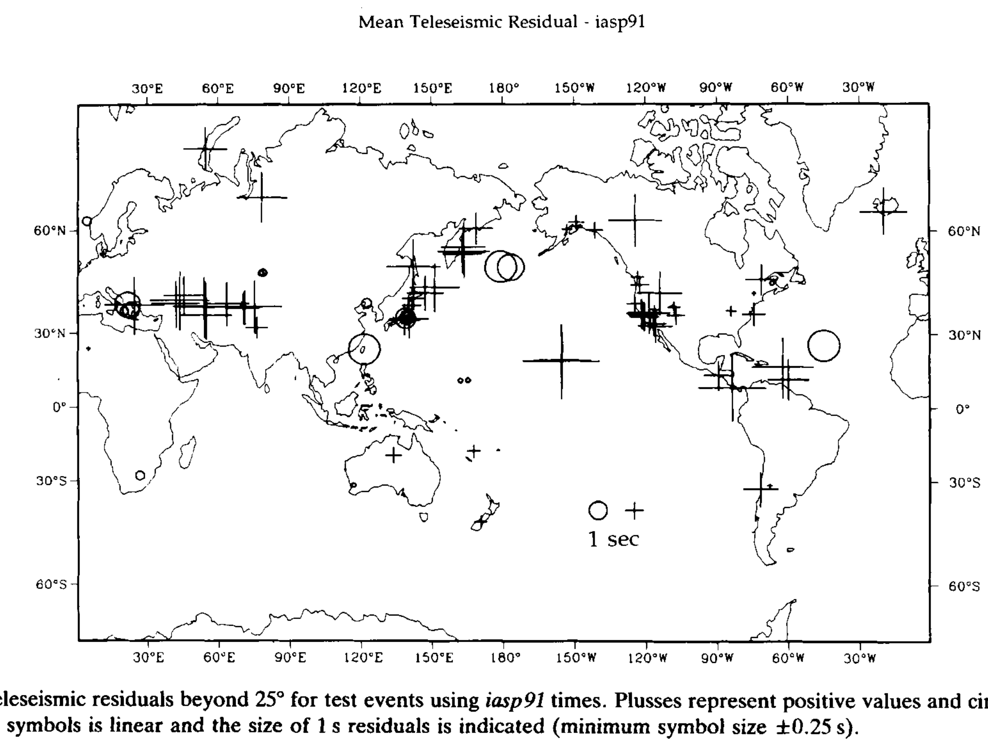

Figure 4. Mean teleseismic residuals beyond 25° for test events using *iasp91* times. Plusses represent positive values and circles negative values. The scaling of the symbols is linear and the size of 1 s residuals is indicated (minimum symbol size ±0.25 s).

Table 4. Location parameters for well-constrained explosions.

		Res. bias > 25°	Orig time bias	Mislocation Azimuth	km
South Pacific					
1954 02 28	Castle Bravo	0.00	-0.06	296.5	7.42
1954 05 04	Castle Yankee	-0.02	-0.15	311.8	9.94
1958 06 28	Oak	-0.01	-0.02	266.9	4.14
Nevada Test Site					
1963 09 13	Bilby	0.10	-0.42	1.9	13.10
1967 05 20	Commodore	0.20	-0.59	18.7	9.96
1968 01 19	Faultless	0.52	-0.83	63.3	9.16
1968 04 26	Boxcar	0.19	-0.59	36.2	11.55
1988 07 07	Alamo	0.44	-0.91	33.1	12.99
Alaska					
1971 11 06	Cannikin	-1.75	1.36	352.1	27.32
Other U.S.A.					
1969 09 10	Rulison (CO)	0.68	-0.56	267.6	5.17
1973 05 17	Rio Blanco (CO)	0.12	-0.57	65.4	13.09
1967 12 10	Gasbuggy (NM)	0.98	-1.20	59.1	5.62
1965 07 15	Chase (VA)	1.26	-1.46	22.0	11.61
Sahara					
1963 10 20		0.03	-0.32	19.3	9.85
1965 02 27		0.18	-0.34	30.7	6.57
E. Kazakh					
1969 11 30		-0.42	0.49	74.8	4.69
1971 04 25		-0.19	0.31	68.0	7.46
1972 08 16		-0.30	0.51	74.5	8.75
1972 11 02		-0.39	0.57	78.5	9.53

as JB and less than the other models we have tried. A more detailed discussion of the location results for the test events will be presented in Engdahl & Buland (1991). The influence of the higher velocity slab for events in subduction zones shows up clearly, since the midlocation vectors point in the direction of subduction.

The arrival time data sets for the test events are rich in later phases and this enables us to supplement the location results, which primarily depend on teleseismic *P*, with an assessment of the general performance of the *iasp91* tables. In Fig. 6 we display the traveltime curves for the *iasp91* model superimposed on the traveltimes for the 57655 phases reported for the test events (corrected to surface focus). The agreement between the observed and calculated times is very encouraging, especially for the later phases.

In Figs 7–9, we display more detailed comparisons for

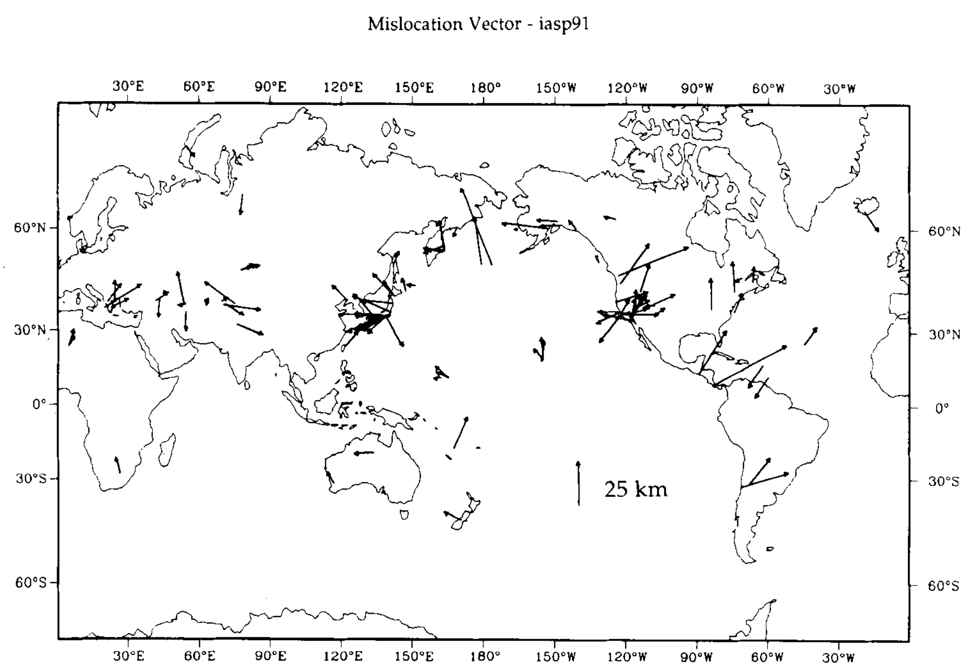

Figure 5. Mislocation vectors at constrained depth for test events using *iasp91* times and teleseismic arrivals.

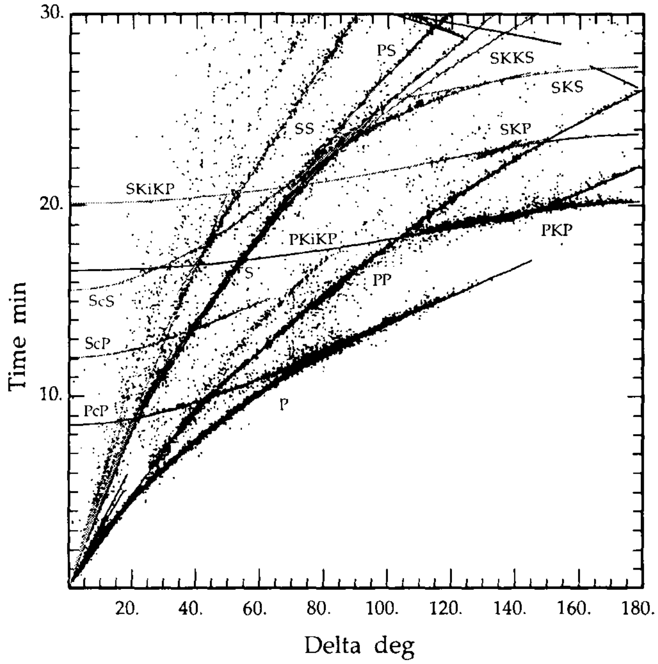

Figure 6. Display of *iasp91* traveltimes superimposed on the times of phases for the test events corrected to surface focus.

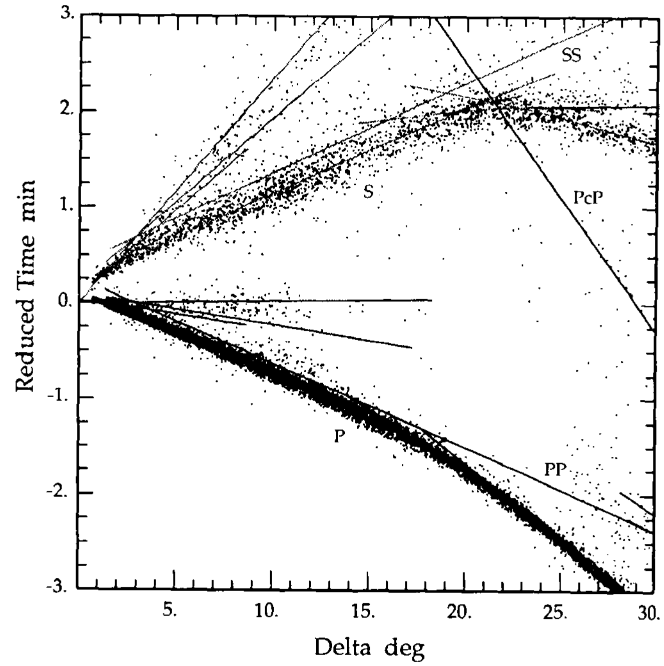

Figure 7. Reduced time display (reduction slowness 19.0 s deg^{-1}) for upper mantle phases from the test event data, corrected to surface focus, compared with *iasp91* times.

important classes of arrivals. Fig. 7 shows the result for both *P* and *S* times out to 30°, covering the distance span for energy return from the upper mantle. It is in this distance range that we would anticipate the greatest level of regional variation and so significant deviations from the computed times could be expected. Nevertheless the correspondence between the complex traveltime curves for the upper mantle branches in the *iasp91* times, and the times from the test events is good for both *P*- and *S*-waves.

Teleseismic *P*- and *S*-wave times for the test events are compared to the *iasp91* table results in Fig. 8. There is a tendency for the calculated *P* times to lie near the leading edge of the cloud of *P* observations. This may arise in part from observations of emergent phases and also to the

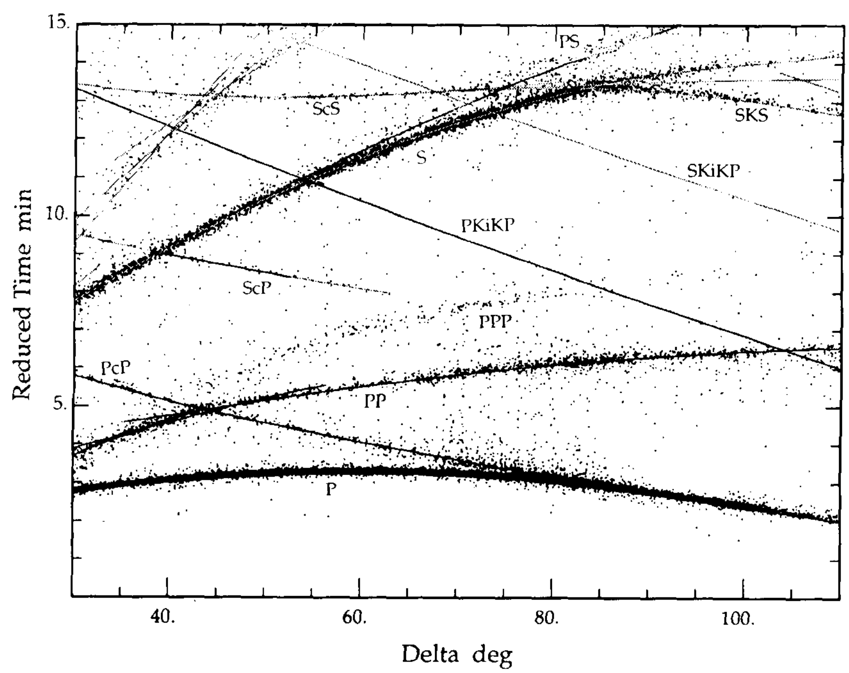

Figure 8. Reduced time display (reduction slowness 6.84 s deg^{-1}) for teleseismic *P* and *S* and associated phases for the test event data, corrected to surface focus, compared with *iasp91* times.

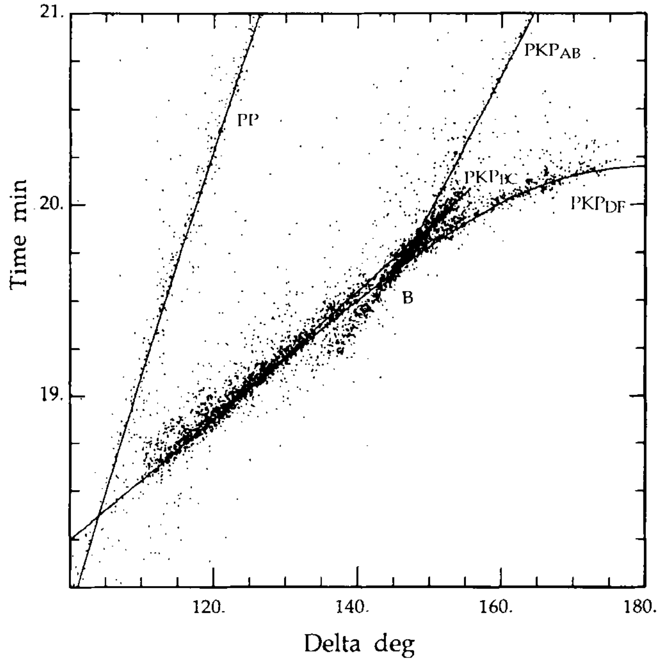

Figure 9. Time display for *PKP* phases from the test event data, corrected to surface focus, compared with *iasp91* times.

difficulty of separating *pP* and *P* arrivals for shallow phases. A more likely explanation (Engdahl & Buland 1991) is that many of the origin times associated with earthquakes in the test event data set may have been estimated using the JB tables. For *S*, the reported phases are more sparse, but agree with the calculated times. The new tables also fit well with the other phases displayed in the time window of Fig. 8, especially for *PcP, PP, ScP* and *ScS*.

The final comparison in Fig. 9 is for the core phase *PKP* which is well represented for the test events. The DF branch is clear over the interval 110° to 130° and beyond 145°. The position of the B caustic predicted by the *iasp91* tables fits well with the observations, and the AB branch is also well constrained. The *PP* phase is less heavily represented but also agrees well with the theoretical predictions.

COMPARISONS WITH OTHER TRAVELTIME TABLES

In Appendix A we present summary traveltime tables for the *iasp91* velocity model for the phases *P, PcP, PKP* and *S, ScS, SKS* for a variety of source depths. Also in Appendix C we illustrate the output from the computational software developed for the new tables displaying many phases at a single epicentral distance. A direct comparison of the new tables against existing tabulations is presented in Figs 10 and 11.

P-waves

In Fig. 10 we display the residuals from the *iasp91* tables, for the Jeffreys & Bullen (1940) tables and the 1968 *P*-tables (Herrin 1968) for surface focus events. As we would expect there is considerable variability out to 30° because neither of the other tables corresponds to the level of complexity of the *iasp91* model in the upper mantle transition zone. The Herrin model is completely smooth in the upper mantle, whilst the JB times correspond to a sharp change in velocity gradient near 400 km depth.

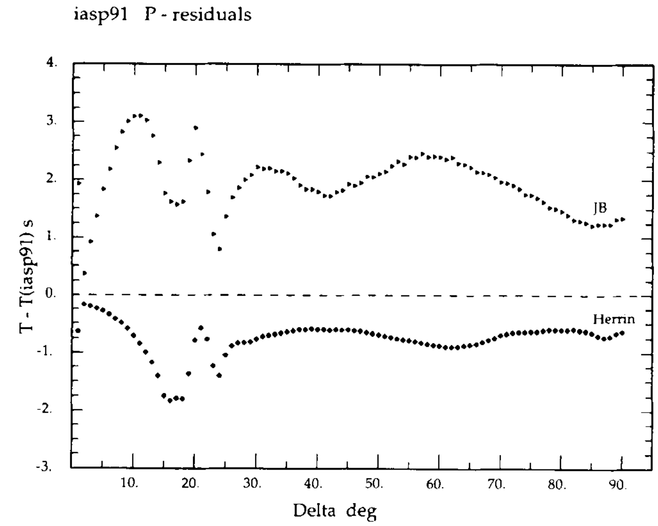

Figure 10. *P*-wave time residuals for other traveltime tables relative to *iasp91*.

Beyond 30°, however, we see that the situation is more stable. The offset of the *iasp91* tables from the Herrin (1968) tables varies by no more than 0.3 s over the entire range from 30° to 95°, with a mean of 0.7 s. The *iasp91* tables for teleseismic *P* can therefore be regarded as roughly equivalent to the Herrin (1968) tables with a baseline shift of 0.7 s. The baseline for *iasp91* is supported by the results from the well-located explosions from around the world in the test event data set.

The behaviour of the JB teleseismic residuals is more complex and suggests a difference in tilt as well as offset. The mean offset between the *iasp91* and JB times is approximately 1.85 s, which is close to the value of 2 s which has often been adopted as an empirical correction to the Jeffreys & Bullen (1940) tables.

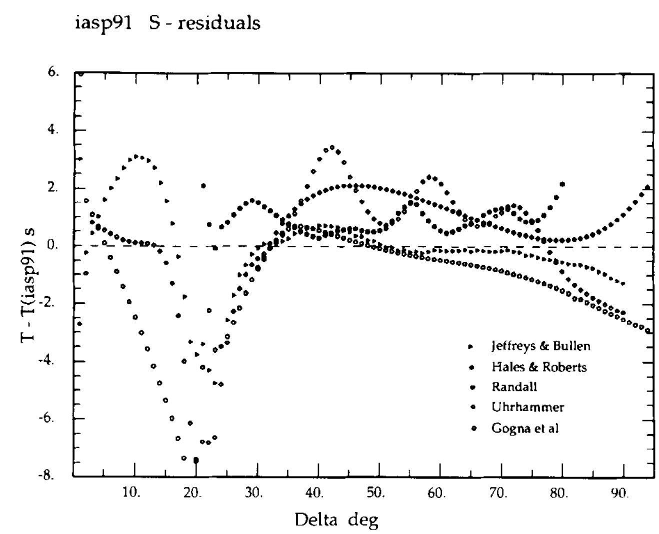

Figure 11. *S*-wave time residuals for other traveltime tables relative to *iasp91*.

S-waves

The residuals of a number of *S*-wave traveltime tables with respect to the new *iasp91* tables are displayed in Fig. 11. We see that for teleseismic *S* there is general agreement between the different tables in a zone about 3 s wide, at least out to the zone of interference between *S* and *SKS* near 80°. The agreement between the different *S* tables evaporates for ranges less than 30° where it is clear that there are very strong regional influences on *S*-wave times. The principal guide for the construction of the *iasp91* times for *S* returns from the upper mantle was the Dziewonski & Anderson (1981) summary traveltimes derived from the ISC data base (see Table 3). These times appear to be more representative of tectonic zones than other regions. This bias is likely to arise from the preponderence of earthquakes and seismic recording stations in such tectonic zones. Randall's (1971) times derived using the same events as the 1968 *P*-tables (Herrin 1968) are just a little slower than *iasp91* from 20° out. The *S* times for central Asian events reported by Gogna *et al.* (1980) are up to 8 s faster.

For the purpose of establishing a teleseismic baseline for *S*, the most interesting set of tables is that of Uhrhammer (1978). He read the *S–P* times for 11 events with the object of minimizing the influence of origin time errors; the *S* times plotted in Fig. 11 are those published for use with the Herrin (1968) *P* times. The rather oscillatory nature of the Uhrhammer residuals compared with the other curves is rather disconcerting but may arise from the limited number of events which were used in the construction of the traveltime table.

In the teleseismic interval the *iasp91* times are quite similar to JB (although the derivation was independent). There is a slight difference in slope from the tables of Hales & Roberts (1970) and Gogna *et al.* (1980). Although not displayed in Fig. 11, there is also a similar level of fit to the *SKS* times of Hales & Roberts (1970).

When we take account of the limitations of *S* observations, the *iasp91* tables give a satisfactory representation of the observed behaviour.

DISCUSSION

Jeffreys (1970, section 3.19) has indicated that he thought that it would not be feasible to make substantial improvements to the Jeffreys & Bullen (1940) tables for global location, but that there would be a need for regional tables. As discussed above the *iasp91* model has been constructed in a way which should make the inclusion of regional models for crustal and upper mantle structure reasonably easy. The requirements for the inclusion of regionalized structure in order to provide a satisfactory tie to the teleseismic times are discussed in Appendix D.

A weakness of the present inversions of traveltimes for mantle and core structure is that the constraints on a number of key phases are relatively weak. For example, observations of *ScP* and *SKP* would improve the tie between the *P* and *S* baselines. We hope that the *iasp91* traveltimes will provide an effective description of the main later-arriving seismic phases, so that accurate phase associations can be made for the time picks reported by seismic observatories. Such improved association routines coupled with current initiatives to collect more traveltime data for later phases (the ISOP project) should provide the information required for more refined traveltime inversion and the delineation of lateral heterogeneity. The strongest influence is likely to arise on the *S* velocity in the mantle and the *P* velocity in the core. The level of agreement between recent studies of the mantle *P*-wave velocities from traveltimes (e.g. Morelli & Dziewonski 1989; Inoue *et al.* 1990; this study) suggest that these are already well constrained.

The ideal procedure for determining earth structure from the ISC data set would be a simultaneous inversion for source location and velocity structure, but this would represent a formidable computational problem. In order to reduce local structural effects, data from many events are currently combined to produce composite rays with a time characteristic of the region. For a simultaneous inversion, this procedure would not be feasible and a full 3-D earth model would be required with each event treated separately.

ACKNOWLEDGMENTS

The development of these *iasp91* traveltime tables has involved many people and we are very appreciative of the help we have received. The contributions of the participants in the 1988 and 1989 workshops have been very valuable and have helped to shape the development of the tables. In particular we would like to thank Anton Hales; without his suggestions, probing questions and untiring enthusiasm it is unlikely that the project would have reached this point. Ray Buland has responded with equanimity to our requests for software modification and has produced a very powerful software package for traveltime computation. Lane Johnson provided considerable help in the early stages of work on the traveltimes for the upper mantle. Ken Toy, Andrea Morelli and Adam Dziewonski generated lower mantle and core models for the workshop at the IASPEI General Assembly in Turkey in 1989 but are not to blame for the final form of the tables. Mike Shimshoni offered useful criticisms of an earlier form of the traveltime tables. Rob van der Hilst undertook a major study of events in the northwest Pacific using a preliminary form of the velocity model which helped shape the final form of the model. We would also like to thank Unesco, IASPEI and the US Air Force Geophysical Laboratory for financial support towards the 1988 and 1989 workshops and the costs of producing the tables. Finally we would like to acknowledge our debt to Harold Jeffreys and Keith Bullen, whose painstaking and arduous work produced a magnificent set of traveltime tables which have served for 50 years.

REFERENCES

Azbel, I. Ya & Yanovskaya, T. B., 1972. Approximations of velocity distributions for calculations of *P*-wave times and amplitudes, *Computational Seismology*, ed. Keilis-Borok, V. I., Consultants Bureau, New York.

Bocharov, V. S., Zelentsev, A. & Mikhailov, V. N., 1989. Characteristics of 96 underground nuclear explosions at the Semipalatinsk test site, *Atomnaya Energiya*, **67**, 3 (in Russian).

Buland, R. & Chapman, C. H., 1983. The computation of seismic travel times, *Bull. seism. Soc. Am.*, **73**, 1271–1302.

Cummins, P. & Johnson, L. R., 1989. Short-period body wave

constraints on properties of the Earth's inner core boundary, *J. geophys. Res.*, **93,** 9058–9074.
Dzeiwonski, A. M. & Anderson, D. L., 1981. Preliminary Reference Earth Model, *Phys. Earth planet Inter.*, **25,** 297–356.
Dzeiwonski, A. M. & Anderson, D. L., 1983. Travel times and station corrections for P waves at teleseismic distances, *J. geophys. Res.* **88,** 3295–3314.
Dziewonski, A. M., Hales, A. L. & Lapwood, E. R., 1975. Parametrically simple Earth models consistent with geophysical data, *Phys. Earth planet. Inter.*, **10,** 12–48.
Engdahl, E. R. & Gunst, R. H., 1966. Use of a high speed computer for the preliminary determination of earthquake epicentres, *Bull. seism. Soc. Am.*, **56,** 325–336.
Engdahl, E. R. & Buland, R., 1991. Tests of seismic travel-time tables with well constrained hypocentres of earthquakes and explosions, *Geophys. J. Int.*, submitted.
Gogna, M. L., Jeffreys, H. & Shimshoni, M., 1980. Seismic travel times from central Asian epicentres, *Geophys. J. R. astr. Soc.*, **63,** 577–599.
Hales, A. L. & Roberts, J. L., 1970. The travel times of S and SKS, *Bull. seism. Soc. Am.*, **60,** 461–489.
Herrin, E., 1968. Introduction to '1968 Seismological Tables for P-phases', *Bull. seism. Soc. Am.*, **58,** 1193–1195.
Inoue, H., Fukao, Y., Tanabe, K. & Ogata, Y., 1990. Whole mantle P-wave travel time tomography, *Phys. Earth planet. Inter.*, **59,** 294–328.
Jeffreys, H., 1932. An alternative to the rejection of observations, *Proc R. Soc. Lond.*, A, **137,** 78–87.
Jeffreys, H., 1939. *Theory of Probability*, Oxford University Press, Oxford.
Jeffreys, H., 1970. *The Earth*, 5th edn, Cambridge University Press, Cambridge.
Jeffreys, H. & Bullen, K. E., 1940. *Seismological Tables*, British Association for the Advancement of Science, London.
Kennett, B. L. N., 1988. Quakes to have better locations, *EOS, Trans. Am. geophys. Un.*, **69,** 1571.
Morelli, A. & Dziewonski, A. M., 1989. Spherically symmetric P- and S-wave velocity models derived from ISC travel times, *Abstracts 25th General Assembly IASPEI*, Istanbul, Turkey.
Randall, M. J., 1971. A revised travel-time table for *S*, *Geophys. J. R. astr. Soc.*, **22,** 229–234.
Revenaugh, J. S. & Jordan, T. H., 1989. A study of mantle layering beneath the western Pacific, *J. geophys. Res.*, **94,** 5787–5813.
Toy, K., 1989a. Tomographic analysis of ISC travel time data for Earth structure, *PhD thesis*, University of California, San Diego.
Toy, K., 1989b. P- and S-wave lower-mantle and core seismic velocity models and station corrections from ISC travel time data, *Abstracts 25th General Assembly IASPEI*, Istanbul, Turkey.
Uhrhammer, R., 1978. *S*-wave travel times for a spherically averaged earth, *Geophys. J. R. astr. Soc.*, **55,** 283–309.
Vergino, E. S., 1989. Soviet test yields, *EOS, Trans. Am. geophys. Un.*, **70,** 1511.
Zielhuis, A., 1988. A shear velocity model for Europe from ISC delay times, *Proceedings of the 4th Workshop on the European Geotraverse Project*, pp. 57–62, European Science Foundation, Strasbourg.

APPENDIX A

Summary traveltime tables for the *iasp91* model

We present here summary traveltime tables at 2° intervals for the phases *P, PcP, PKPab, PKPbc, PKPdf* and *S, ScS, SKSac, SKSdf* for a variety of source depths. These tables have been extracted from the output of the standard computational procedure described in Appendix C.

For each distance we display the traveltime for each of the depths as a value in minutes and seconds and beneath in italics the slowness ($dT/d\Delta$) for that distance.

These traveltime tables have been produced from the tau-spline routines by a computer routine which assembles the results for the requisite depths and then generates table formatting commands which allow the production of direct laserprinter output.

Note added in proof

A more comprehensive set of traveltime tables (the *IASPEI 1991 Seismological Tables*) has also been prepared using the *iasp91* computational routines and is available from Bibliotech, ANUtech Pty Ltd, GPO Box 4, Canberra ACT 2601, Australia (A$19 including postage and packing).

These extended tables present traveltimes at 1° sampling in range for body waves (for a wide range of depths), core phases and converted phases. Differential times for surface reflected phases (*pP–P, sP–P, sS–S, pS–S*) are also tabulated.

In addition, at 2° intervals the traveltimes and slowness are tabulated for a wide range of phases for source depths of 0 100, 300 and 600 km. Ellipticity corrections are provided for major phases.

Table A1. Summary traveltime tables.

P

Δ	Depth of source [km] 0.	35.	70.	150.	250.	400.	550.	700.
	m s	m s	m s	m s	m s	m s	m s	m s
0.0	0 00.00	0 05.76	0 10.11	0 20.03	0 32.11	0 49.32	1 05.02	1 19.70
	19.17	*0.00*	*0.00*	*0.00*	*0.00*	*0.00*	*0.00*	*0.00*
2.0	0 35.03	0 31.27	0 31.62	0 35.08	0 42.42	0 55.91	1 09.62	1 23.13
	13.75	*13.75*	*13.46*	*11.63*	*9.01*	*6.19*	*4.43*	*3.33*
4.0	1 02.53	0 58.77	0 58.81	1 00.20	1 03.75	1 12.03	1 21.79	1 32.55
	13.75	*13.75*	*13.65*	*13.06*	*11.72*	*9.48*	*7.46*	*5.93*
6.0	1 30.01	1 26.25	1 26.14	1 26.65	1 28.08	1 32.56	1 38.54	1 46.23
	13.74	*13.73*	*13.67*	*13.32*	*12.46*	*10.86*	*9.10*	*7.61*
8.0	1 57.47	1 53.70	1 53.47	1 53.33	1 53.24	1 54.92	1 57.65	2 02.49
	13.72	*13.72*	*13.66*	*13.34*	*12.65*	*11.41*	*9.90*	*8.55*
10.0	2 24.90	2 21.12	2 20.79	2 19.93	2 18.51	2 17.52	2 17.84	2 20.09
	13.70	*13.70*	*13.65*	*13.24*	*12.59*	*11.08*	*10.24*	*8.98*
12.0	2 52.27	2 48.48	2 48.06	2 46.19	2 43.52	2 39.62	2 38.44	2 38.18
	13.68	*13.67*	*13.62*	*13.00*	*12.40*	*11.01*	*10.33*	*9.08*
14.0	3 19.59	3 15.79	3 14.95	3 11.81	3 08.06	3 01.54	2 59.09	2 56.34
	13.65	*13.64*	*13.12*	*12.61*	*12.13*	*10.89*	*10.30*	*9.07*
16.0	3 46.38	3 42.32	3 40.66	3 36.64	3 30.73	3 23.17	3 19.44	3 14.44
	12.92	*12.81*	*12.57*	*12.22*	*10.97*	*10.73*	*9.19*	*9.03*
18.0	4 11.58	4 07.34	4 04.98	3 59.15	3 52.52	3 44.43	3 37.77	3 32.42
	12.33	*12.26*	*11.00*	*10.93*	*10.81*	*10.53*	*9.14*	*8.95*
20.0	4 34.10	4 29.49	4 26.83	4 20.83	4 13.93	4 04.34	3 55.97	3 50.24
	10.90	*10.88*	*10.84*	*10.74*	*10.59*	*9.15*	*9.06*	*8.87*
22.0	4 55.71	4 51.05	4 48.31	4 42.09	4 33.89	4 22.56	4 13.99	4 07.92
	10.70	*10.67*	*10.62*	*10.50*	*9.14*	*9.07*	*8.95*	*8.81*
24.0	5 16.31	5 11.33	5 08.08	5 00.74	4 52.08	4 40.60	4 31.79	4 25.48
	9.14	*9.13*	*9.12*	*9.09*	*9.06*	*8.96*	*8.86*	*8.74*
26.0	5 34.51	5 29.51	5 26.24	5 18.83	5 10.08	4 58.42	4 49.44	4 42.87
	9.06	*9.05*	*9.03*	*8.99*	*8.93*	*8.86*	*8.79*	*8.65*
28.0	5 52.50	5 47.49	5 44.18	5 36.70	5 27.85	5 16.08	5 06.94	5 00.08
	8.93	*8.92*	*8.91*	*8.88*	*8.85*	*8.79*	*8.70*	*8.56*
30.0	6 10.27	6 05.24	6 01.92	5 54.38	5 45.48	5 33.58	5 24.25	5 17.09
	8.85	*8.84*	*8.83*	*8.81*	*8.77*	*8.70*	*8.60*	*8.45*
32.0	6 27.89	6 22.85	6 19.50	6 11.92	6 02.93	5 50.89	5 41.34	5 33.89
	8.77	*8.76*	*8.75*	*8.72*	*8.68*	*8.60*	*8.49*	*8.34*
34.0	6 45.34	6 40.27	6 36.90	6 29.25	6 20.18	6 07.97	5 58.21	5 50.46
	8.67	*8.66*	*8.65*	*8.61*	*8.57*	*8.48*	*8.38*	*8.23*
36.0	7 02.57	6 57.49	6 54.08	6 46.36	6 37.20	6 24.82	6 14.83	6 06.79
	8.56	*8.55*	*8.53*	*8.50*	*8.45*	*8.36*	*8.25*	*8.11*
38.0	7 19.56	7 14.46	7 11.02	7 03.23	6 53.97	6 41.42	6 31.21	6 22.89
	8.44	*8.43*	*8.41*	*8.37*	*8.32*	*8.23*	*8.12*	*7.99*
40.0	7 36.30	7 31.18	7 27.71	7 19.85	7 10.48	6 57.76	6 47.33	6 38.73
	8.30	*8.29*	*8.28*	*8.24*	*8.19*	*8.10*	*7.99*	*7.86*
42.0	7 52.78	7 47.63	7 44.13	7 36.19	7 26.73	7 13.83	7 03.19	6 54.32
	8.17	*8.16*	*8.14*	*8.10*	*8.06*	*7.97*	*7.86*	*7.73*
44.0	8 08.98	8 03.81	8 00.28	7 52.26	7 42.70	7 29.63	7 18.78	7 09.66
	8.03	*8.02*	*8.00*	*7.97*	*7.92*	*7.83*	*7.73*	*7.60*
46.0	8 24.90	8 19.71	8 16.15	8 08.06	7 58.39	7 45.16	7 34.10	7 24.74
	7.89	*7.88*	*7.86*	*7.83*	*7.78*	*7.70*	*7.59*	*7.47*
48.0	8 40.54	8 35.33	8 31.73	8 23.57	8 13.81	8 00.41	7 49.16	7 39.55
	7.75	*7.74*	*7.72*	*7.68*	*7.64*	*7.55*	*7.46*	*7.34*
50.0	8 55.89	8 50.66	8 47.03	8 38.80	8 28.94	8 15.38	8 03.94	7 54.10
	7.60	*7.59*	*7.58*	*7.54*	*7.49*	*7.42*	*7.32*	*7.21*

Table A1. (*continued*)

P

Δ	Depth of source [km] 0.	35.	70.	150.	250.	400.	550.	700.
	m s	m s	m s	m s	m s	m s	m s	m s
50.0	8 55.89	8 50.66	8 47.03	8 38.80	8 28.94	8 15.38	8 03.94	7 54.10
	7.60	*7.59*	*7.58*	*7.54*	*7.49*	*7.42*	*7.32*	*7.21*
52.0	9 10.95	9 05.70	9 02.04	8 53.74	8 43.78	8 30.08	8 18.44	8 08.39
	7.46	*7.45*	*7.43*	*7.40*	*7.35*	*7.28*	*7.18*	*7.08*
54.0	9 25.72	9 20.45	9 16.76	9 08.39	8 58.35	8 44.49	8 32.68	8 22.41
	7.31	*7.30*	*7.29*	*7.26*	*7.21*	*7.14*	*7.05*	*6.94*
56.0	9 40.20	9 34.91	9 31.19	9 22.76	9 12.63	8 58.62	8 46.64	8 36.17
	7.17	*7.16*	*7.14*	*7.11*	*7.07*	*7.00*	*6.91*	*6.81*
58.0	9 54.39	9 49.08	9 45.34	9 36.84	9 26.62	9 12.48	9 00.32	8 49.65
	7.02	*7.01*	*7.00*	*6.97*	*6.93*	*6.86*	*6.77*	*6.68*
60.0	10 08.29	10 02.96	9 59.19	9 50.63	9 40.33	9 26.05	9 13.73	9 02.87
	6.88	*6.87*	*6.86*	*6.82*	*6.78*	*6.72*	*6.64*	*6.54*
62.0	10 21.90	10 16.55	10 12.76	10 04.13	9 53.76	9 39.34	9 26.86	9 15.82
	6.73	*6.72*	*6.71*	*6.68*	*6.64*	*6.57*	*6.50*	*6.41*
64.0	10 35.22	10 29.86	10 26.04	10 17.35	10 06.90	9 52.35	9 39.72	9 28.50
	6.59	*6.58*	*6.57*	*6.54*	*6.50*	*6.43*	*6.36*	*6.27*
66.0	10 48.25	10 42.87	10 39.02	10 30.28	10 19.75	10 05.08	9 52.30	9 40.91
	6.44	*6.43*	*6.42*	*6.39*	*6.36*	*6.29*	*6.22*	*6.14*
68.0	11 00.99	10 55.59	10 51.72	10 42.92	10 32.32	10 17.52	10 04.60	9 53.04
	6.30	*6.29*	*6.28*	*6.25*	*6.21*	*6.15*	*6.08*	*6.00*
70.0	11 13.43	11 08.02	11 04.12	10 55.27	10 44.59	10 29.68	10 16.62	10 04.90
	6.15	*6.14*	*6.13*	*6.10*	*6.07*	*6.01*	*5.94*	*5.86*
72.0	11 25.59	11 20.15	11 16.24	11 07.33	10 56.58	10 41.55	10 28.35	10 16.48
	6.00	*5.99*	*5.98*	*5.96*	*5.92*	*5.86*	*5.80*	*5.72*
74.0	11 37.45	11 32.00	11 28.06	11 19.10	11 08.28	10 53.14	10 39.81	10 27.78
	5.86	*5.85*	*5.84*	*5.81*	*5.78*	*5.72*	*5.66*	*5.58*
76.0	11 49.01	11 43.54	11 39.58	11 30.57	11 19.69	11 04.44	10 50.97	10 38.80
	5.71	*5.70*	*5.69*	*5.66*	*5.63*	*5.57*	*5.51*	*5.44*
78.0	12 00.27	11 54.79	11 50.81	11 41.75	11 30.80	11 15.44	11 01.85	10 49.53
	5.56	*5.55*	*5.54*	*5.51*	*5.48*	*5.43*	*5.36*	*5.29*
80.0	12 11.23	12 05.73	12 01.73	11 52.62	11 41.61	11 26.14	11 12.43	10 59.98
	5.40	*5.40*	*5.39*	*5.36*	*5.33*	*5.28*	*5.22*	*5.15*
82.0	12 21.88	12 16.37	12 12.35	12 03.20	11 52.12	11 36.55	11 22.72	11 10.12
	5.25	*5.24*	*5.23*	*5.21*	*5.18*	*5.13*	*5.07*	*5.00*
84.0	12 32.23	12 26.70	12 22.66	12 13.46	12 02.32	11 46.65	11 32.70	11 19.98
	5.09	*5.09*	*5.07*	*5.05*	*5.02*	*4.97*	*4.92*	*4.85*
86.0	12 42.26	12 36.72	12 32.66	12 23.41	12 12.22	11 56.44	11 42.36	11 29.49
	4.94	*4.93*	*4.93*	*4.91*	*4.87*	*4.80*	*4.73*	*4.70*
88.0	12 51.96	12 46.40	12 42.31	12 33.01	12 21.75	12 05.89	11 51.74	11 38.82
	4.74	*4.73*	*4.73*	*4.72*	*4.70*	*4.68*	*4.66*	*4.64*
90.0	13 01.35	12 55.78	12 51.69	12 42.37	12 31.09	12 15.19	12 01.01	11 48.05
	4.66	*4.66*	*4.66*	*4.65*	*4.64*	*4.63*	*4.61*	*4.60*
92.0	13 10.62	13 05.05	13 00.96	12 51.63	12 40.33	12 24.41	12 10.20	11 57.21
	4.61	*4.61*	*4.61*	*4.61*	*4.60*	*4.59*	*4.57*	*4.55*
94.0	13 19.81	13 14.24	13 10.14	13 00.80	12 49.49	12 33.54	12 19.29	12 06.26
	4.58	*4.57*	*4.57*	*4.57*	*4.56*	*4.54*	*4.52*	*4.49*
96.0	13 28.91	13 23.34	13 19.23	13 09.87	12 58.54	12 42.55	12 28.26	12 15.18
	4.52	*4.52*	*4.51*	*4.51*	*4.49*	*4.48*	*4.45*	*4.44*
98.0	13 37.89	13 32.30	13 28.19	13 18.81	13 07.46	12 51.45	12 37.14	12 24.06
	4.45	*4.45*	*4.45*	*4.44*	*4.44*	*4.44*	*4.44*	*4.44*
100.0	13 46.77	13 41.18	13 37.07	13 27.69	13 16.34	13 00.33	12 46.02	12 32.94
	4.44	*4.44*	*4.44*	*4.44*	*4.44*	*4.44*	*4.44*	*4.44*

Table A1. (*continued*)

P	Depth of source [km]							
Δ	0.	35.	70.	150.	250.	400.	550.	700.
	m s	m s	m s	m s	m s	m s	m s	m s
100.0	13 46.77	13 41.18	13 37.07	13 27.69	13 16.34	13 00.33	12 46.02	12 32.94
	4.44	*4.44*	*4.44*	*4.44*	*4.44*	*4.44*	*4.44*	*4.44*
102.0	13 55.64	13 50.06	13 45.94	13 36.57	13 25.21	13 09.21	12 54.90	12 41.82
	4.44	*4.44*	*4.44*	*4.44*	*4.44*	*4.44*	*4.44*	*4.44*
104.0	14 04.52	13 58.94	13 54.82	13 45.45	13 34.09	13 18.08	13 03.78	12 50.69
	4.44	*4.44*	*4.44*	*4.44*	*4.44*	*4.44*	*4.44*	*4.44*
106.0	14 13.40	14 07.82	14 03.70	13 54.33	13 42.97	13 26.96	13 12.65	12 59.57
	4.44	*4.44*	*4.44*	*4.44*	*4.44*	*4.44*	*4.44*	*4.44*
108.0	14 22.28	14 16.70	14 12.58	14 03.20	13 51.85	13 35.84	13 21.53	13 08.45
	4.44	*4.44*	*4.44*	*4.44*	*4.44*	*4.44*	*4.44*	*4.44*
110.0	14 31.16	14 25.57	14 21.46	14 12.08	14 00.73	13 44.72	13 30.41	13 17.33
	4.44	*4.44*	*4.44*	*4.44*	*4.44*	*4.44*	*4.44*	*4.44*
112.0	14 40.03	14 34.45	14 30.33	14 20.96	14 09.60	13 53.60	13 39.29	13 26.21
	4.44	*4.44*	*4.44*	*4.44*	*4.44*	*4.44*	*4.44*	*4.44*
114.0	14 48.91	14 43.33	14 39.21	14 29.84	14 18.48	14 02.47	13 48.17	13 35.08
	4.44	*4.44*	*4.44*	*4.44*	*4.44*	*4.44*	*4.44*	*4.44*
116.0	14 57.79	14 52.21	14 48.09	14 38.71	14 27.36	14 11.35	13 57.04	13 43.96
	4.44	*4.44*	*4.44*	*4.44*	*4.44*	*4.44*	*4.44*	*4.44*
118.0	15 06.67	15 01.08	14 56.97	14 47.59	14 36.24	14 20.23	14 05.92	13 52.84
	4.44	*4.44*	*4.44*	*4.44*	*4.44*	*4.44*	*4.44*	*4.44*
120.0	15 15.54	15 09.96	15 05.84	14 56.47	14 45.12	14 29.11	14 14.80	14 01.72
	4.44	*4.44*	*4.44*	*4.44*	*4.44*	*4.44*	*4.44*	*4.44*
122.0	15 24.42	15 18.84	15 14.72	15 05.35	14 53.99	14 37.98	14 23.68	14 10.59
	4.44	*4.44*	*4.44*	*4.44*	*4.44*	*4.44*	*4.44*	*4.44*
124.0	15 33.30	15 27.72	15 23.60	15 14.23	15 02.87	14 46.86	14 32.55	14 19.47
	4.44	*4.44*	*4.44*	*4.44*	*4.44*	*4.44*	*4.44*	*4.44*
126.0	15 42.18	15 36.60	15 32.48	15 23.10	15 11.75	14 55.74	14 41.43	14 28.35
	4.44	*4.44*	*4.44*	*4.44*	*4.44*	*4.44*	*4.44*	*4.44*
128.0	15 51.06	15 45.47	15 41.36	15 31.98	15 20.63	15 04.62	14 50.31	14 37.23
	4.44	*4.44*	*4.44*	*4.44*	*4.44*	*4.44*	*4.44*	*4.44*
130.0	15 59.93	15 54.35	15 50.23	15 40.86	15 29.50	15 13.50	14 59.19	14 46.11
	4.44	*4.44*	*4.44*	*4.44*	*4.44*	*4.44*	*4.44*	*4.44*
132.0	16 08.81	16 03.23	15 59.11	15 49.74	15 38.38	15 22.37	15 08.07	14 54.98
	4.44	*4.44*	*4.44*	*4.44*	*4.44*	*4.44*	*4.44*	*4.44*
134.0	16 17.69	16 12.11	16 07.99	15 58.62	15 47.26	15 31.25	15 16.94	15 03.86
	4.44	*4.44*	*4.44*	*4.44*	*4.44*	*4.44*	*4.44*	*4.44*
136.0	16 26.57	16 20.98	16 16.87	16 07.49	15 56.14	15 40.13	15 25.82	15 12.74
	4.44	*4.44*	*4.44*	*4.44*	*4.44*	*4.44*	*4.44*	*4.44*
138.0	16 35.44	16 29.86	16 25.74	16 16.37	16 05.02	15 49.01	15 34.70	15 21.62
	4.44	*4.44*	*4.44*	*4.44*	*4.44*	*4.44*	*4.44*	*4.44*
140.0	16 44.32	16 38.74	16 34.62	16 25.25	16 13.89	15 57.88	15 43.58	15 30.49
	4.44	*4.44*	*4.44*	*4.44*	*4.44*	*4.44*	*4.44*	*4.44*

Table A1. *(continued)*

PcP

Δ	Depth of source [km] 0.	35.	70.	150.	250.	400.	550.	700.
	m s	m s	m s	m s	m s	m s	m s	m s
0.0	8 31.28	8 25.52	8 21.17	8 11.25	7 59.17	7 41.96	7 26.26	7 11.58
	0.00	*0.00*	*0.00*	*0.00*	*0.00*	*0.00*	*0.00*	*0.00*
2.0	8 31.47	8 25.72	8 21.37	8 11.45	7 59.37	7 42.16	7 26.46	7 11.79
	0.19	*0.19*	*0.19*	*0.19*	*0.19*	*0.20*	*0.20*	*0.20*
4.0	8 32.05	8 26.29	8 21.94	8 12.03	7 59.95	7 42.75	7 27.06	7 12.40
	0.38	*0.38*	*0.38*	*0.39*	*0.39*	*0.40*	*0.40*	*0.41*
6.0	8 33.01	8 27.26	8 22.91	8 12.99	8 00.93	7 43.74	7 28.06	7 13.41
	0.57	*0.57*	*0.58*	*0.58*	*0.58*	*0.59*	*0.60*	*0.61*
8.0	8 34.35	8 28.60	8 24.25	8 14.34	8 02.29	7 45.11	7 29.45	7 14.83
	0.76	*0.76*	*0.77*	*0.77*	*0.77*	*0.78*	*0.79*	*0.81*
10.0	8 36.06	8 30.31	8 25.97	8 16.07	8 04.03	7 46.87	7 31.23	7 16.64
	0.95	*0.95*	*0.95*	*0.96*	*0.96*	*0.98*	*0.99*	*1.00*
12.0	8 38.14	8 32.40	8 28.06	8 18.17	8 06.14	7 49.01	7 33.40	7 18.83
	1.13	*1.13*	*1.14*	*1.14*	*1.15*	*1.16*	*1.18*	*1.20*
14.0	8 40.59	8 34.85	8 30.52	8 20.64	8 08.63	7 51.52	7 35.94	7 21.41
	1.31	*1.32*	*1.32*	*1.32*	*1.33*	*1.35*	*1.36*	*1.38*
16.0	8 43.39	8 37.66	8 33.33	8 23.47	8 11.47	7 54.40	7 38.85	7 24.37
	1.49	*1.49*	*1.50*	*1.50*	*1.51*	*1.53*	*1.55*	*1.57*
18.0	8 46.54	8 40.81	8 36.49	8 26.65	8 14.67	7 57.63	7 42.13	7 27.68
	1.66	*1.66*	*1.67*	*1.67*	*1.69*	*1.70*	*1.72*	*1.75*
20.0	8 50.04	8 44.31	8 40.00	8 30.17	8 18.21	8 01.21	7 45.74	7 31.35
	1.83	*1.83*	*1.84*	*1.84*	*1.86*	*1.87*	*1.89*	*1.92*
22.0	8 53.86	8 48.14	8 43.83	8 34.02	8 22.08	8 05.12	7 49.70	7 35.36
	1.99	*1.99*	*2.00*	*2.01*	*2.02*	*2.04*	*2.06*	*2.09*
24.0	8 58.00	8 52.28	8 47.99	8 38.19	8 26.28	8 09.36	7 53.99	7 39.70
	2.15	*2.15*	*2.16*	*2.16*	*2.18*	*2.20*	*2.22*	*2.25*
26.0	9 02.45	8 56.74	8 52.45	8 42.67	8 30.79	8 13.91	7 58.58	7 44.35
	2.30	*2.30*	*2.31*	*2.32*	*2.33*	*2.35*	*2.38*	*2.40*
28.0	9 07.20	9 01.50	8 57.21	8 47.46	8 35.60	8 18.76	8 03.48	7 49.31
	2.45	*2.45*	*2.45*	*2.46*	*2.48*	*2.50*	*2.52*	*2.55*
30.0	9 12.23	9 06.54	9 02.26	8 52.53	8 40.69	8 23.90	8 08.68	7 54.56
	2.59	*2.59*	*2.60*	*2.61*	*2.62*	*2.64*	*2.66*	*2.69*
32.0	9 17.55	9 11.85	9 07.59	8 57.87	8 46.06	8 29.31	8 14.14	8 00.09
	2.72	*2.72*	*2.73*	*2.74*	*2.75*	*2.78*	*2.80*	*2.83*
34.0	9 23.12	9 17.44	9 13.18	9 03.48	8 51.70	8 34.99	8 19.87	8 05.88
	2.85	*2.85*	*2.86*	*2.87*	*2.88*	*2.90*	*2.93*	*2.96*
36.0	9 28.95	9 23.27	9 19.02	9 09.34	8 57.59	8 40.92	8 25.85	8 11.92
	2.97	*2.98*	*2.98*	*2.99*	*3.00*	*3.03*	*3.05*	*3.08*
38.0	9 35.01	9 29.34	9 25.10	9 15.44	9 03.71	8 47.09	8 32.07	8 18.19
	3.09	*3.09*	*3.10*	*3.11*	*3.12*	*3.14*	*3.17*	*3.20*
40.0	9 41.30	9 35.64	9 31.40	9 21.77	9 10.06	8 53.48	8 38.52	8 24.70
	3.20	*3.20*	*3.21*	*3.22*	*3.23*	*3.25*	*3.28*	*3.30*
42.0	9 47.81	9 42.15	9 37.93	9 28.31	9 16.63	9 00.09	8 45.17	8 31.41
	3.31	*3.31*	*3.31*	*3.32*	*3.34*	*3.36*	*3.38*	*3.41*
44.0	9 54.52	9 48.87	9 44.65	9 35.05	9 23.40	9 06.90	8 52.03	8 38.32
	3.40	*3.41*	*3.41*	*3.42*	*3.43*	*3.45*	*3.48*	*3.50*
46.0	10 01.43	9 55.78	9 51.57	9 41.99	9 30.36	9 13.90	8 59.08	8 45.41
	3.50	*3.50*	*3.51*	*3.51*	*3.53*	*3.55*	*3.57*	*3.59*
48.0	10 08.51	10 02.87	9 58.67	9 49.10	9 37.49	9 21.07	9 06.30	8 52.69
	3.59	*3.59*	*3.59*	*3.60*	*3.61*	*3.63*	*3.65*	*3.68*
50.0	10 15.76	10 10.13	10 05.93	9 56.38	9 44.80	9 28.42	9 13.68	9 00.12
	3.67	*3.67*	*3.67*	*3.68*	*3.69*	*3.71*	*3.73*	*3.76*

Table A1. (*continued*)

PcP	Depth of source [km]							
Δ	0.	35.	70.	150.	250.	400.	550.	700.
	m s	m s	m s	m s	m s	m s	m s	m s
50.0	10 15.76	10 10.13	10 05.93	9 56.38	9 44.80	9 28.42	9 13.68	9 00.12
	3.67	*3.67*	*3.67*	*3.68*	*3.69*	*3.71*	*3.73*	*3.76*
52.0	10 23.18	10 17.55	10 13.36	10 03.83	9 52.26	9 35.91	9 21.22	9 07.70
	3.74	*3.75*	*3.75*	*3.76*	*3.77*	*3.79*	*3.81*	*3.83*
54.0	10 30.74	10 25.11	10 20.93	10 11.42	9 59.87	9 43.56	9 28.90	9 15.43
	3.82	*3.82*	*3.82*	*3.83*	*3.84*	*3.86*	*3.87*	*3.90*
56.0	10 38.44	10 32.82	10 28.65	10 19.14	10 07.62	9 51.33	9 36.71	9 23.28
	3.88	*3.89*	*3.89*	*3.90*	*3.90*	*3.92*	*3.94*	*3.96*
58.0	10 46.27	10 40.65	10 36.49	10 27.00	10 15.49	9 59.23	9 44.65	9 31.26
	3.95	*3.95*	*3.95*	*3.96*	*3.97*	*3.98*	*4.00*	*4.01*
60.0	10 54.22	10 48.61	10 44.44	10 34.97	10 23.48	10 07.25	9 52.70	9 39.34
	4.00	*4.01*	*4.01*	*4.01*	*4.02*	*4.03*	*4.05*	*4.07*
62.0	11 02.28	10 56.67	10 52.51	10 43.05	10 31.57	10 15.37	10 00.85	9 47.53
	4.06	*4.06*	*4.06*	*4.07*	*4.07*	*4.09*	*4.10*	*4.12*
64.0	11 10.44	11 04.83	11 00.68	10 51.23	10 39.77	10 23.59	10 09.10	9 55.80
	4.10	*4.11*	*4.11*	*4.11*	*4.12*	*4.13*	*4.15*	*4.16*
66.0	11 18.70	11 13.09	11 08.94	10 59.50	10 48.06	10 31.90	10 17.43	10 04.17
	4.15	*4.15*	*4.15*	*4.16*	*4.16*	*4.18*	*4.19*	*4.20*
68.0	11 27.04	11 21.43	11 17.29	11 07.86	10 56.42	10 40.29	10 25.84	10 12.60
	4.19	*4.19*	*4.19*	*4.20*	*4.20*	*4.21*	*4.22*	*4.24*
70.0	11 35.45	11 29.85	11 25.71	11 16.29	11 04.87	10 48.75	10 34.32	10 21.11
	4.23	*4.23*	*4.23*	*4.23*	*4.24*	*4.25*	*4.26*	*4.27*
72.0	11 43.94	11 38.34	11 34.21	11 24.79	11 13.38	10 57.28	10 42.87	10 29.68
	4.26	*4.26*	*4.26*	*4.27*	*4.27*	*4.28*	*4.29*	*4.30*
74.0	11 52.49	11 46.89	11 42.76	11 33.35	11 21.95	11 05.86	10 51.47	10 38.30
	4.29	*4.29*	*4.29*	*4.30*	*4.30*	*4.31*	*4.32*	*4.32*
76.0	12 01.09	11 55.50	11 51.37	11 41.97	11 30.57	11 14.50	11 00.13	10 46.97
	4.32	*4.32*	*4.32*	*4.32*	*4.32*	*4.33*	*4.34*	*4.35*
78.0	12 09.75	12 04.16	12 00.03	11 50.63	11 39.25	11 23.19	11 08.83	10 55.69
	4.34	*4.34*	*4.34*	*4.34*	*4.35*	*4.35*	*4.36*	*4.37*
80.0	12 18.45	12 12.86	12 08.73	11 59.34	11 47.96	11 31.91	11 17.56	11 04.44
	4.36	*4.36*	*4.36*	*4.36*	*4.37*	*4.37*	*4.38*	*4.38*
82.0	12 27.19	12 21.60	12 17.47	12 08.09	11 56.71	11 40.67	11 26.33	11 13.22
	4.38	*4.38*	*4.38*	*4.38*	*4.38*	*4.39*	*4.39*	*4.40*
84.0	12 35.96	12 30.37	12 26.25	12 16.86	12 05.49	11 49.46	11 35.13	11 22.03
	4.39	*4.39*	*4.39*	*4.40*	*4.40*	*4.40*	*4.41*	*4.41*
86.0	12 44.75	12 39.17	12 35.05	12 25.67	12 14.30	11 58.28	11 43.95	11 30.85
	4.41	*4.41*	*4.41*	*4.41*	*4.41*	*4.41*	*4.42*	*4.42*
88.0	12 53.58	12 47.99	12 43.87	12 34.49	12 23.13	12 07.11	11 52.79	11 39.70
	4.42	*4.42*	*4.42*	*4.42*	*4.42*	*4.42*	*4.42*	*4.43*
90.0	13 02.42	12 56.83	12 52.71	12 43.34	12 31.98	12 15.96	12 01.65	11 48.56
	4.42	*4.43*	*4.43*	*4.43*	*4.43*	*4.43*	*4.43*	*4.43*
92.0	13 11.27	13 05.69	13 01.57	12 52.19	12 40.84	12 24.83	12 10.51	11 57.43
	4.43	*4.43*	*4.43*	*4.43*	*4.43*	*4.43*	*4.43*	*4.44*
94.0	13 20.14	13 14.56	13 10.44	13 01.06	12 49.71	12 33.70	12 19.39	12 06.30
	4.43	*4.43*	*4.43*	*4.44*	*4.44*	*4.44*	*4.44*	*4.44*
96.0	13 29.01	13 23.43	13 19.31	13 09.94	12 58.58	12 42.57	12 28.27	
	4.44	*4.44*	*4.44*	*4.44*	*4.44*	*4.44*	*4.44*	
98.0	13 37.89	13 32.31	13 28.19					
	4.44	*4.44*	*4.44*					

Table A1. (*continued*)

PKPab

Δ	Depth of source [km] 0.	35.	70.	150.	250.	400.	550.	700.
	m s	m s	m s	m s	m s	m s	m s	m s
146.0	19 41.54	19 35.91	19 31.74	19 22.24	19 10.72	18 54.45	18 39.87	18 26.50
	3.87	*3.87*	*3.88*	*3.91*	*3.93*	*3.97*	*4.01*	*4.06*
148.0	19 49.45	19 43.83	19 39.67	19 30.21	19 18.73	19 02.53	18 48.01	18 34.71
	4.03	*4.03*	*4.04*	*4.05*	*4.07*	*4.09*	*4.12*	*4.15*
150.0	19 57.61	19 52.00	19 47.85	19 38.41	19 26.96	19 10.80	18 56.33	18 43.08
	4.13	*4.13*	*4.14*	*4.14*	*4.16*	*4.18*	*4.20*	*4.22*
152.0	20 05.94	20 00.34	19 56.20	19 46.77	19 35.34	19 19.22	19 04.78	18 51.57
	4.20	*4.20*	*4.20*	*4.21*	*4.22*	*4.24*	*4.25*	*4.27*
154.0	20 14.40	20 08.80	20 04.67	19 55.25	19 43.84	19 27.74	19 13.33	19 00.15
	4.26	*4.26*	*4.26*	*4.26*	*4.27*	*4.28*	*4.30*	*4.31*
156.0	20 22.95	20 17.36	20 13.23	20 03.82	19 52.42	19 36.34	19 21.96	19 08.80
	4.30	*4.30*	*4.30*	*4.30*	*4.31*	*4.32*	*4.33*	*4.34*
158.0	20 31.58	20 25.99	20 21.86	20 12.46	20 01.07	19 45.01	19 30.65	19 17.51
	4.33	*4.33*	*4.33*	*4.34*	*4.34*	*4.35*	*4.36*	*4.37*
160.0	20 40.27	20 34.68	20 30.56	20 21.16	20 09.78	19 53.74	19 39.39	19 26.26
	4.36	*4.36*	*4.36*	*4.36*	*4.37*	*4.37*	*4.38*	*4.39*
162.0	20 49.01	20 43.42	20 39.30	20 29.91	20 18.54	20 02.50	19 48.16	19 35.05
	4.38	*4.38*	*4.38*	*4.38*	*4.39*	*4.39*	*4.40*	*4.40*
164.0	20 57.79	20 52.20	20 48.08	20 38.70	20 27.33	20 11.30	19 56.97	19 43.87
	4.40	*4.40*	*4.40*	*4.40*	*4.40*	*4.41*	*4.41*	*4.41*
166.0	21 06.60	21 01.01	20 56.89	20 47.51	20 36.15	20 20.12	20 05.80	19 52.71
	4.41	*4.41*	*4.41*	*4.41*	*4.41*	*4.42*	*4.42*	*4.42*
168.0	21 15.43	21 09.84	21 05.72	20 56.35	20 44.99	20 28.97	20 14.65	20 01.56
	4.42	*4.42*	*4.42*	*4.42*	*4.42*	*4.43*	*4.43*	*4.43*
170.0	21 24.28	21 18.69	21 14.58	21 05.20	20 53.84	20 37.83	20 23.52	20 10.43
	4.43	*4.43*	*4.43*	*4.43*	*4.43*	*4.43*	*4.43*	*4.43*
172.0	21 33.14	21 27.56	21 23.44	21 14.06	21 02.71	20 46.70	20 32.39	20 19.31
	4.43	*4.43*	*4.43*	*4.43*	*4.43*	*4.44*	*4.44*	*4.44*
174.0	21 42.01	21 36.43	21 32.31	21 22.94	21 11.58	20 55.57	20 41.26	20 28.18
	4.44	*4.44*	*4.44*	*4.44*	*4.44*	*4.44*	*4.44*	*4.44*
176.0	21 50.89	21 45.31	21 41.19	21 31.81	21 20.46	20 55.57	20 41.26	20 28.18
	4.44	*4.44*	*4.44*	*4.44*	*4.44*	*4.44*	*4.44*	*4.44*
178.0	21 50.89	21 45.31	21 41.19	21 31.81	21 20.46	20 55.57	20 41.26	20 28.18
	4.44	*4.44*	*4.44*	*4.44*	*4.44*	*4.44*	*4.44*	*4.44*
180.0	21 50.89	21 45.31	21 41.19	21 31.81	21 20.46	20 55.57	20 41.26	20 28.18
	4.44	*4.44*	*4.44*	*4.44*	*4.44*	*4.44*	*4.44*	*4.44*

PKPbc

Δ	Depth of source [km] 0.	35.	70.	150.	250.	400.	550.	700.
	m s	m s	m s	m s	m s	m s	m s	m s
146.0	19 40.79	19 35.11	19 30.87	19 21.20	19 09.45	18 52.76	18 37.64	18 23.61
	3.07	*3.06*	*3.05*	*3.02*	*2.99*	*2.94*	*2.88*	*2.83*
148.0	19 46.63	19 40.94	19 36.68	19 26.97	19 15.16	18 58.39	18 43.18	18 29.04
	2.79	*2.78*	*2.77*	*2.76*	*2.73*	*2.70*	*2.66*	*2.62*
150.0	19 51.98	19 46.28	19 42.00	19 32.26	19 20.41	19 03.58	18 48.29	18 34.08
	2.57	*2.56*	*2.56*	*2.54*	*2.53*	*2.50*	*2.46*	*2.43*
152.0	19 56.92	19 51.21	19 46.92	19 37.15	19 25.27	19 08.38	18 53.04	18 38.77
	2.38	*2.37*	*2.37*	*2.35*	*2.34*	*2.31*	*2.29*	*2.26*
154.0	20 01.49	19 55.77	19 51.48	19 41.69	19 29.78	19 12.84	18 57.45	18 43.12
	2.20	*2.20*	*2.19*	*2.18*	*2.17*	*2.15*	*2.12*	*2.09*

Table A1. (*continued*)

PKPdf	Depth of source [km]							
Δ	0.	35.	70.	150.	250.	400.	550.	700.
	m s	m s	m s	m s	m s	m s	m s	m s
114.0	18 40.84	18 35.11	18 30.81	18 20.98	18 09.03	17 52.04	17 36.59	17 22.20
	1.91	*1.91*	*1.91*	*1.91*	*1.91*	*1.91*	*1.91*	*1.91*
116.0	18 44.67	18 38.94	18 34.64	18 24.81	18 12.86	17 55.87	17 40.42	17 26.03
	1.91	*1.91*	*1.91*	*1.91*	*1.91*	*1.91*	*1.91*	*1.91*
118.0	18 48.50	18 42.77	18 38.46	18 28.64	18 16.69	17 59.70	17 44.25	17 29.85
	1.91	*1.91*	*1.91*	*1.91*	*1.91*	*1.91*	*1.91*	*1.91*
120.0	18 52.32	18 46.60	18 42.29	18 32.47	18 20.52	18 03.53	17 48.07	17 33.68
	1.91	*1.91*	*1.91*	*1.91*	*1.91*	*1.91*	*1.91*	*1.91*
122.0	18 56.14	18 50.42	18 46.11	18 36.29	18 24.34	18 07.34	17 51.89	17 37.49
	1.91	*1.91*	*1.91*	*1.91*	*1.91*	*1.91*	*1.91*	*1.91*
124.0	18 59.96	18 54.23	18 49.92	18 40.10	18 28.15	18 11.16	17 55.70	17 41.30
	1.90	*1.90*	*1.90*	*1.90*	*1.90*	*1.90*	*1.90*	*1.90*
126.0	19 03.76	18 58.04	18 53.73	18 43.90	18 31.95	18 14.96	17 59.50	17 45.10
	1.90	*1.90*	*1.90*	*1.90*	*1.90*	*1.90*	*1.90*	*1.90*
128.0	19 07.55	19 01.83	18 57.52	18 47.69	18 35.74	18 18.75	18 03.29	17 48.89
	1.89	*1.89*	*1.89*	*1.89*	*1.89*	*1.89*	*1.89*	*1.89*
130.0	19 11.33	19 05.61	19 01.29	18 51.47	18 39.52	18 22.52	18 07.05	17 52.65
	1.88	*1.88*	*1.88*	*1.88*	*1.88*	*1.88*	*1.88*	*1.88*
132.0	19 15.09	19 09.36	19 05.05	18 55.22	18 43.27	18 26.27	18 10.80	17 56.40
	1.87	*1.87*	*1.87*	*1.87*	*1.87*	*1.87*	*1.87*	*1.87*
134.0	19 18.82	19 13.09	19 08.78	18 58.95	18 47.00	18 29.99	18 14.52	18 00.11
	1.86	*1.86*	*1.86*	*1.86*	*1.86*	*1.86*	*1.85*	*1.85*
136.0	19 22.52	19 16.80	19 12.48	19 02.65	18 50.69	18 33.69	18 18.21	18 03.80
	1.84	*1.84*	*1.84*	*1.84*	*1.84*	*1.84*	*1.83*	*1.83*
138.0	19 26.19	19 20.46	19 16.15	19 06.31	18 54.35	18 37.34	18 21.86	18 07.44
	1.82	*1.82*	*1.82*	*1.82*	*1.82*	*1.82*	*1.81*	*1.81*
140.0	19 29.80	19 24.08	19 19.76	19 09.93	18 57.96	18 40.94	18 25.46	18 11.03
	1.79	*1.79*	*1.79*	*1.79*	*1.79*	*1.79*	*1.78*	*1.78*
142.0	19 33.36	19 27.63	19 23.32	19 13.48	19 01.51	18 44.49	18 28.99	18 14.55
	1.76	*1.76*	*1.76*	*1.76*	*1.76*	*1.75*	*1.75*	*1.75*
144.0	19 36.85	19 31.12	19 26.81	19 16.97	19 04.99	18 47.96	18 32.45	18 18.00
	1.73	*1.73*	*1.72*	*1.72*	*1.72*	*1.72*	*1.71*	*1.71*
146.0	19 40.26	19 34.53	19 30.21	19 20.37	19 08.39	18 51.34	18 35.83	18 21.37
	1.68	*1.68*	*1.68*	*1.68*	*1.67*	*1.67*	*1.66*	*1.66*
148.0	19 43.57	19 37.84	19 33.52	19 23.67	19 11.68	18 54.63	18 39.10	18 24.62
	1.63	*1.63*	*1.62*	*1.62*	*1.62*	*1.61*	*1.61*	*1.60*
150.0	19 46.77	19 41.03	19 36.71	19 26.85	19 14.86	18 57.79	18 42.25	18 27.76
	1.57	*1.56*	*1.56*	*1.56*	*1.56*	*1.55*	*1.54*	*1.53*
152.0	19 49.83	19 44.09	19 39.76	19 29.90	19 17.90	19 00.82	18 45.27	18 30.76
	1.50	*1.49*	*1.49*	*1.49*	*1.49*	*1.48*	*1.47*	*1.46*
154.0	19 52.74	19 47.00	19 42.67	19 32.80	19 20.80	19 03.70	18 48.13	18 33.60
	1.42	*1.41*	*1.41*	*1.41*	*1.41*	*1.40*	*1.39*	*1.38*
156.0	19 55.49	19 49.75	19 45.41	19 35.54	19 23.52	19 06.42	18 50.83	18 36.29
	1.33	*1.33*	*1.33*	*1.33*	*1.32*	*1.31*	*1.30*	*1.30*
158.0	19 58.06	19 52.31	19 47.98	19 38.10	19 26.07	19 08.95	18 53.35	18 38.79
	1.24	*1.24*	*1.24*	*1.23*	*1.23*	*1.22*	*1.21*	*1.20*
160.0	20 00.43	19 54.69	19 50.35	19 40.47	19 28.43	19 11.30	18 55.68	18 41.10
	1.14	*1.14*	*1.14*	*1.13*	*1.13*	*1.12*	*1.12*	*1.11*
162.0	20 02.61	19 56.86	19 52.52	19 42.63	19 30.59	19 13.44	18 57.81	18 43.21
	1.04	*1.03*	*1.03*	*1.03*	*1.03*	*1.02*	*1.01*	*1.01*
164.0	20 04.58	19 58.83	19 54.49	19 44.59	19 32.54	19 15.38	18 59.73	18 45.12
	0.93	*0.93*	*0.93*	*0.92*	*0.92*	*0.92*	*0.91*	*0.90*

Table A1. (*continued*)

PKPdf	Depth of source [km]							
Δ	0.	35.	70.	150.	250.	400.	550.	700.
	m s	m s	m s	m s	m s	m s	m s	m s
164.0	20 04.58	19 58.83	19 54.49	19 44.59	19 32.54	19 15.38	18 59.73	18 45.12
	0.93	*0.93*	*0.93*	*0.92*	*0.92*	*0.92*	*0.91*	*0.90*
166.0	20 06.32	20 00.57	19 56.23	19 46.33	19 34.27	19 17.10	19 01.44	18 46.81
	0.82	*0.82*	*0.82*	*0.81*	*0.81*	*0.81*	*0.80*	*0.79*
168.0	20 07.85	20 02.10	19 57.75	19 47.84	19 35.78	19 18.60	19 02.93	18 48.29
	0.71	*0.70*	*0.70*	*0.70*	*0.70*	*0.69*	*0.69*	*0.68*
170.0	20 09.15	20 03.39	19 59.05	19 49.13	19 37.07	19 19.88	19 04.20	18 49.55
	0.59	*0.59*	*0.59*	*0.59*	*0.58*	*0.58*	*0.58*	*0.57*
172.0	20 10.21	20 04.46	20 00.11	19 50.19	19 38.12	19 20.93	19 05.24	18 50.58
	0.47	*0.47*	*0.47*	*0.47*	*0.47*	*0.47*	*0.46*	*0.46*
174.0	20 11.04	20 05.29	20 00.94	19 51.02	19 38.94	19 21.74	19 06.05	18 51.38
	0.36	*0.36*	*0.36*	*0.35*	*0.35*	*0.35*	*0.35*	*0.34*
176.0	20 11.64	20 05.88	20 01.53	19 51.61	19 39.53	19 22.33	19 06.63	18 51.96
	0.24	*0.24*	*0.24*	*0.24*	*0.24*	*0.23*	*0.23*	*0.23*
178.0	20 12.00	20 06.24	20 01.89	19 51.97	19 39.89	19 22.68	19 06.98	18 52.30
	0.12	*0.12*	*0.12*	*0.12*	*0.12*	*0.12*	*0.12*	*0.12*
180.0	20 12.12	20 06.36	20 02.01	19 52.09	19 40.01	19 22.80	19 07.09	18 52.42
	0.00	*0.00*	*0.00*	*0.00*	*0.00*	*0.00*	*0.00*	*0.00*

Table A1. (*continued*)

S	Depth of source [km]							
Δ	0.	35.	70.	150.	250.	400.	550.	700.
	m s	m s	m s	m s	m s	m s	m s	m s
0.0	0 00.00	0 09.95	0 17.77	0 35.57	0 57.64	1 29.42	1 58.31	2 25.04
	33.09	*0.01*	*0.00*	*0.00*	*0.00*	*0.00*	*0.00*	*0.00*
2.0	1 01.73	0 55.60	0 56.21	1 02.46	1 16.25	1 41.43	2 06.72	2 31.29
	24.74	*24.73*	*24.17*	*20.82*	*16.26*	*11.27*	*8.10*	*6.08*
4.0	1 51.19	1 45.05	1 45.03	1 47.49	1 54.82	2 10.82	2 28.96	2 48.49
	24.72	*24.71*	*24.51*	*23.43*	*21.24*	*17.31*	*13.65*	*10.83*
6.0	2 40.59	2 34.44	2 34.09	2 34.96	2 39.01	2 48.41	2 59.63	3 13.46
	24.68	*24.67*	*24.53*	*23.93*	*22.68*	*19.91*	*16.68*	*13.88*
8.0	3 29.91	3 23.73	3 23.12	3 22.99	3 24.94	3 29.48	3 34.67	3 43.11
	24.63	*24.62*	*24.49*	*24.07*	*23.17*	*21.01*	*18.16*	*15.58*
10.0	4 19.10	4 12.90	4 12.05	4 11.17	4 11.43	4 11.36	4 11.72	4 15.09
	24.56	*24.55*	*24.43*	*24.10*	*23.26*	*20.46*	*18.78*	*16.25*
12.0	5 08.14	5 01.90	5 00.83	4 59.34	4 57.78	4 52.13	4 49.48	4 47.75
	24.48	*24.46*	*24.34*	*24.07*	*23.05*	*20.30*	*18.93*	*16.34*
14.0	5 56.99	5 50.71	5 49.42	5 47.44	5 43.50	5 32.46	5 27.27	5 20.33
	24.37	*24.34*	*24.25*	*24.02*	*22.65*	*20.02*	*18.82*	*16.22*
16.0	6 45.62	6 39.29	6 37.86	6 35.31	6 26.48	6 12.14	6 03.10	5 52.55
	24.26	*24.25*	*24.18*	*23.01*	*20.18*	*19.64*	*16.51*	*15.92*
18.0	7 34.06	7 27.71	7 26.13	7 18.48	7 06.47	6 50.95	6 35.87	6 24.25
	24.18	*24.17*	*24.09*	*20.09*	*19.79*	*19.17*	*16.25*	*15.80*
20.0	8 20.86	8 13.18	8 08.59	7 58.24	7 45.56	7 24.87	7 07.99	6 55.77
	20.05	*19.99*	*19.90*	*19.64*	*19.28*	*16.27*	*15.86*	*15.73*
22.0	9 00.49	8 52.68	8 47.87	8 35.27	8 19.16	7 57.00	7 39.61	7 27.16
	19.55	*19.48*	*19.35*	*16.33*	*16.20*	*15.86*	*15.76*	*15.66*
24.0	9 35.41	9 26.88	9 20.97	9 07.54	8 51.09	8 28.61	8 11.07	7 58.40
	16.20	*16.17*	*16.11*	*15.88*	*15.82*	*15.76*	*15.70*	*15.57*
26.0	10 07.31	9 58.71	9 52.71	9 39.18	9 22.65	9 00.06	8 42.39	8 29.42
	15.82	*15.81*	*15.80*	*15.77*	*15.74*	*15.69*	*15.62*	*15.45*
28.0	10 38.86	10 30.25	10 24.23	10 10.65	9 54.06	9 31.38	9 13.51	9 00.21
	15.74	*15.73*	*15.72*	*15.70*	*15.67*	*15.61*	*15.50*	*15.32*
30.0	11 10.27	11 01.64	10 55.60	10 41.98	10 25.32	10 02.48	9 44.38	9 30.72
	15.67	*15.66*	*15.65*	*15.62*	*15.57*	*15.49*	*15.37*	*15.18*
32.0	11 41.51	11 32.86	11 26.80	11 13.10	10 56.35	10 33.34	10 14.98	10 00.93
	15.57	*15.56*	*15.54*	*15.50*	*15.45*	*15.36*	*15.23*	*15.03*
34.0	12 12.52	12 03.85	11 57.75	11 43.98	11 27.11	11 03.90	10 45.28	10 30.83
	15.44	*15.43*	*15.41*	*15.37*	*15.31*	*15.21*	*15.07*	*14.87*
36.0	12 43.26	12 34.56	12 28.43	12 14.56	11 57.57	11 34.15	11 15.25	11 00.40
	15.30	*15.28*	*15.26*	*15.22*	*15.15*	*15.04*	*14.90*	*14.70*
38.0	13 13.69	13 04.96	12 58.79	12 44.83	12 27.71	12 04.07	11 44.86	11 29.62
	15.13	*15.12*	*15.10*	*15.05*	*14.98*	*14.87*	*14.72*	*14.52*
40.0	13 43.79	13 35.03	13 28.81	13 14.75	12 57.50	12 33.62	12 14.12	11 58.48
	14.96	*14.94*	*14.92*	*14.87*	*14.80*	*14.69*	*14.53*	*14.34*
42.0	14 13.52	14 04.73	13 58.47	13 44.30	13 26.91	13 02.80	12 43.00	12 26.96
	14.77	*14.76*	*14.73*	*14.68*	*14.61*	*14.49*	*14.34*	*14.15*
44.0	14 42.87	14 34.05	14 27.74	14 13.47	13 55.94	13 31.60	13 11.49	12 55.07
	14.58	*14.56*	*14.54*	*14.49*	*14.42*	*14.30*	*14.15*	*13.96*
46.0	15 11.84	15 02.98	14 56.63	14 42.24	14 24.57	13 59.99	13 39.59	13 22.79
	14.38	*14.36*	*14.34*	*14.29*	*14.22*	*14.10*	*13.95*	*13.76*
48.0	15 40.39	15 31.50	15 25.10	15 10.61	14 52.80	14 27.98	14 07.28	13 50.11
	14.17	*14.16*	*14.13*	*14.08*	*14.01*	*13.89*	*13.74*	*13.56*
50.0	16 08.53	15 59.61	15 53.16	15 38.56	15 20.61	14 55.55	14 34.56	14 17.03
	13.96	*13.95*	*13.92*	*13.87*	*13.80*	*13.68*	*13.54*	*13.36*

Table A1. (*continued*)

S

	Depth of source [km]							
Δ	0.	35.	70.	150.	250.	400.	550.	700.
	m s	m s	m s	m s	m s	m s	m s	m s
50.0	16 08.53	15 59.61	15 53.16	15 38.56	15 20.61	14 55.55	14 34.56	14 17.03
	13.96	*13.95*	*13.92*	*13.87*	*13.80*	*13.68*	*13.54*	*13.36*
52.0	16 36.24	16 27.29	16 20.79	16 06.09	15 47.99	15 22.71	15 01.43	14 43.55
	13.75	*13.73*	*13.71*	*13.65*	*13.59*	*13.47*	*13.33*	*13.16*
54.0	17 03.52	16 54.54	16 48.00	16 33.18	16 14.95	15 49.44	15 27.88	15 09.66
	13.53	*13.52*	*13.49*	*13.44*	*13.37*	*13.26*	*13.12*	*12.95*
56.0	17 30.37	17 21.35	17 14.77	16 59.85	16 41.48	16 15.74	15 53.91	15 35.35
	13.31	*13.30*	*13.28*	*13.22*	*13.16*	*13.04*	*12.91*	*12.74*
58.0	17 56.78	17 47.73	17 41.10	17 26.08	17 07.57	16 41.61	16 19.51	16 00.62
	13.09	*13.08*	*13.05*	*13.00*	*12.94*	*12.83*	*12.69*	*12.53*
60.0	18 22.74	18 13.66	18 06.98	17 51.86	17 33.22	17 07.04	16 44.68	16 25.48
	12.87	*12.85*	*12.83*	*12.78*	*12.72*	*12.61*	*12.48*	*12.32*
62.0	18 48.25	18 39.14	18 32.42	18 17.20	17 58.43	17 32.04	17 09.42	16 49.90
	12.64	*12.63*	*12.61*	*12.56*	*12.49*	*12.39*	*12.26*	*12.11*
64.0	19 13.31	19 04.17	18 57.41	18 42.09	18 23.19	17 56.59	17 33.72	17 13.90
	12.42	*12.40*	*12.38*	*12.33*	*12.27*	*12.16*	*12.04*	*11.89*
66.0	19 37.92	19 28.74	19 21.94	19 06.52	18 47.50	18 20.69	17 57.57	17 37.46
	12.19	*12.17*	*12.15*	*12.10*	*12.04*	*11.94*	*11.82*	*11.67*
68.0	20 02.07	19 52.86	19 46.02	19 30.50	19 11.36	18 44.35	18 20.99	18 00.58
	11.96	*11.94*	*11.92*	*11.88*	*11.81*	*11.71*	*11.59*	*11.45*
70.0	20 25.75	20 16.52	20 09.63	19 54.02	19 34.76	19 07.55	18 43.94	18 23.26
	11.73	*11.71*	*11.69*	*11.65*	*11.58*	*11.48*	*11.37*	*11.23*
72.0	20 48.97	20 39.70	20 32.78	20 17.08	19 57.69	19 30.28	19 06.45	18 45.49
	11.49	*11.48*	*11.45*	*11.41*	*11.35*	*11.25*	*11.14*	*11.00*
74.0	21 11.71	21 02.42	20 55.46	20 39.66	20 20.16	19 52.56	19 28.49	19 07.27
	11.25	*11.24*	*11.22*	*11.17*	*11.12*	*11.02*	*10.91*	*10.77*
76.0	21 33.98	21 24.65	21 17.66	21 01.77	20 42.15	20 14.36	19 50.07	19 28.58
	11.01	*11.00*	*10.98*	*10.93*	*10.88*	*10.78*	*10.67*	*10.54*
78.0	21 55.76	21 46.41	21 39.37	21 23.40	21 03.67	20 35.69	20 11.17	19 49.42
	10.77	*10.76*	*10.74*	*10.69*	*10.64*	*10.54*	*10.43*	*10.30*
80.0	22 17.05	22 07.67	22 00.60	21 44.53	21 24.69	20 56.52	20 31.79	20 09.79
	10.52	*10.51*	*10.49*	*10.44*	*10.39*	*10.30*	*10.19*	*10.06*
82.0	22 37.84	22 28.43	22 21.32	22 05.17	21 45.22	21 16.87	20 51.92	20 29.66
	10.27	*10.26*	*10.24*	*10.19*	*10.14*	*10.05*	*9.94*	*9.81*
84.0	22 58.12	22 48.69	22 41.54	22 25.30	22 05.24	21 36.71	21 11.54	20 49.03
	10.01	*10.00*	*9.98*	*9.94*	*9.88*	*9.79*	*9.68*	*9.56*
86.0	23 17.88	23 08.42	23 01.23	22 44.91	22 24.73	21 56.02	21 30.65	21 07.90
	9.74	*9.73*	*9.71*	*9.67*	*9.62*	*9.53*	*9.42*	*9.30*
88.0	23 37.10	23 27.61	23 20.39	23 03.99	22 43.70	22 14.81	21 49.23	21 26.24
	9.48	*9.46*	*9.44*	*9.40*	*9.35*	*9.26*	*9.15*	*9.04*
90.0	23 55.78	23 46.26	23 39.00	23 22.52	23 02.12	22 33.06	22 07.27	21 44.03
	9.20	*9.19*	*9.17*	*9.13*	*9.07*	*8.99*	*8.88*	*8.77*
92.0	24 13.90	24 04.35	23 57.06	23 40.49	23 19.98	22 50.75	22 24.80	22 01.45
	8.91	*8.90*	*8.88*	*8.84*	*8.78*	*8.73*	*8.69*	*8.66*
94.0	24 31.47	24 21.90	24 14.59	23 57.97	23 37.41	23 08.11	22 42.09	22 18.64
	8.70	*8.70*	*8.69*	*8.68*	*8.66*	*8.63*	*8.59*	*8.52*
96.0	24 48.78	24 39.20	24 31.87	24 15.22	23 54.62	23 25.24	22 59.11	22 35.52
	8.60	*8.59*	*8.58*	*8.56*	*8.53*	*8.48*	*8.43*	*8.36*
98.0	25 05.81	24 56.22	24 48.87	24 32.17	24 11.51	23 42.03	23 15.81	22 52.17
	8.43	*8.43*	*8.42*	*8.39*	*8.36*	*8.32*	*8.32*	*8.32*
100.0	25 22.52	25 12.93	25 05.57	24 48.85	24 28.17	23 58.68	23 32.46	23 08.82
	8.32	*8.32*	*8.32*	*8.32*	*8.32*	*8.32*	*8.32*	*8.32*

Table A1. (*continued*)

S				Depth of source [km]				
Δ	**0.**	**35.**	**70.**	**150.**	**250.**	**400.**	**550.**	**700.**
	m s	m s	m s	m s	m s	m s	m s	m s
100.0	25 22.52	25 12.93	25 05.57	24 48.85	24 28.17	23 58.68	23 32.46	23 08.82
	8.32	*8.32*	*8.32*	*8.32*	*8.32*	*8.32*	*8.32*	*8.32*
102.0	25 39.17	25 29.57	25 22.21	25 05.49	24 44.81	24 15.33	23 49.11	23 25.46
	8.32	*8.32*	*8.32*	*8.32*	*8.32*	*8.32*	*8.32*	*8.32*
104.0	25 55.82	25 46.22	25 38.86	25 22.14	25 01.46	24 31.97	24 05.75	23 42.11
	8.32	*8.32*	*8.32*	*8.32*	*8.32*	*8.32*	*8.32*	*8.32*
106.0	26 12.46	26 02.86	25 55.51	25 38.79	25 18.11	24 48.62	24 22.40	23 58.76
	8.32	*8.32*	*8.32*	*8.32*	*8.32*	*8.32*	*8.32*	*8.32*
108.0	26 29.11	26 19.51	26 12.15	25 55.43	25 34.75	25 05.27	24 39.05	24 15.40
	8.32	*8.32*	*8.32*	*8.32*	*8.32*	*8.32*	*8.32*	*8.32*
110.0	26 45.76	26 36.16	26 28.80	26 12.08	25 51.40	25 21.91	24 55.69	24 32.05
	8.32	*8.32*	*8.32*	*8.32*	*8.32*	*8.32*	*8.32*	*8.32*
112.0	27 02.40	26 52.80	26 45.44	26 28.73	26 08.05	25 38.56	25 12.34	24 48.70
	8.32	*8.32*	*8.32*	*8.32*	*8.32*	*8.32*	*8.32*	*8.32*
114.0	27 19.05	27 09.45	27 02.09	26 45.37	26 24.69	25 55.21	25 28.99	25 05.34
	8.32	*8.32*	*8.32*	*8.32*	*8.32*	*8.32*	*8.32*	*8.32*
116.0	27 35.70	27 26.10	27 18.74	27 02.02	26 41.34	26 11.85	25 45.63	25 21.99
	8.32	*8.32*	*8.32*	*8.32*	*8.32*	*8.32*	*8.32*	*8.32*
118.0	27 52.34	27 42.74	27 35.38	27 18.67	26 57.99	26 28.50	26 02.28	25 38.64
	8.32	*8.32*	*8.32*	*8.32*	*8.32*	*8.32*	*8.32*	*8.32*
120.0	28 08.99	27 59.39	27 52.03	27 35.31	27 14.63	26 45.14	26 18.93	25 55.28
	8.32	*8.32*	*8.32*	*8.32*	*8.32*	*8.32*	*8.32*	*8.32*
122.0	28 25.64	28 16.04	28 08.68	27 51.96	27 31.28	27 01.79	26 35.57	26 11.93
	8.32	*8.32*	*8.32*	*8.32*	*8.32*	*8.32*	*8.32*	*8.32*
124.0	28 42.28	28 32.68	28 25.32	28 08.60	27 47.93	27 18.44	26 52.22	26 28.58
	8.32	*8.32*	*8.32*	*8.32*	*8.32*	*8.32*	*8.32*	*8.32*
126.0	28 58.93	28 49.33	28 41.97	28 25.25	28 04.57	27 35.08	27 08.87	26 45.22
	8.32	*8.32*	*8.32*	*8.32*	*8.32*	*8.32*	*8.32*	*8.32*
128.0	29 15.57	29 05.98	28 58.62	28 41.90	28 21.22	27 51.73	27 25.51	27 01.87
	8.32	*8.32*	*8.32*	*8.32*	*8.32*	*8.32*	*8.32*	*8.32*
130.0	29 32.22	29 22.62	29 15.26	28 58.54	28 37.87	28 08.38	27 42.16	27 18.52
	8.32	*8.32*	*8.32*	*8.32*	*8.32*	*8.32*	*8.32*	*8.32*
132.0	29 48.87	29 39.27	29 31.91	29 15.19	28 54.51	28 25.02	27 58.81	27 35.16
	8.32	*8.32*	*8.32*	*8.32*	*8.32*	*8.32*	*8.32*	*8.32*
134.0	30 05.51	29 55.92	29 48.56	29 31.84	29 11.16	28 41.67	28 15.45	27 51.81
	8.32	*8.32*	*8.32*	*8.32*	*8.32*	*8.32*	*8.32*	*8.32*
136.0	30 22.16	30 12.56	30 05.20	29 48.48	29 27.80	28 58.32	28 32.10	28 08.46
	8.32	*8.32*	*8.32*	*8.32*	*8.32*	*8.32*	*8.32*	*8.32*
138.0	30 38.81	30 29.21	30 21.85	30 05.13	29 44.45	29 14.96	28 48.74	28 25.10
	8.32	*8.32*	*8.32*	*8.32*	*8.32*	*8.32*	*8.32*	*8.32*
140.0	30 55.45	30 45.86	30 38.50	30 21.78	30 01.10	29 31.61	29 05.39	28 41.75
	8.32	*8.32*	*8.32*	*8.32*	*8.32*	*8.32*	*8.32*	*8.32*

Table A1. (*continued*)

ScS — Depth of source [km]

Δ	0.	35.	70.	150.	250.	400.	550.	700.
	m s	m s	m s	m s	m s	m s	m s	m s
0.0	15 35.57	15 25.62	15 17.80	15 00.01	14 37.93	14 06.16	13 37.26	13 10.53
	0.00	*0.00*	*0.00*	*0.00*	*0.00*	*0.00*	*0.00*	*0.00*
2.0	15 35.93	15 25.98	15 18.16	15 00.36	14 38.29	14 06.52	13 37.63	13 10.91
	0.35	*0.35*	*0.36*	*0.36*	*0.36*	*0.37*	*0.37*	*0.38*
4.0	15 36.99	15 27.04	15 19.22	15 01.44	14 39.37	14 07.61	13 38.74	13 12.03
	0.71	*0.71*	*0.71*	*0.71*	*0.72*	*0.73*	*0.74*	*0.75*
6.0	15 38.76	15 28.81	15 21.00	15 03.22	14 41.17	14 09.43	13 40.58	13 13.90
	1.06	*1.06*	*1.06*	*1.07*	*1.08*	*1.09*	*1.10*	*1.12*
8.0	15 41.22	15 31.28	15 23.47	15 05.71	14 43.67	14 11.96	13 43.15	13 16.51
	1.41	*1.41*	*1.41*	*1.42*	*1.43*	*1.45*	*1.47*	*1.49*
10.0	15 44.38	15 34.45	15 26.65	15 08.90	14 46.88	14 15.21	13 46.44	13 19.85
	1.75	*1.75*	*1.76*	*1.77*	*1.78*	*1.80*	*1.82*	*1.85*
12.0	15 48.22	15 38.29	15 30.50	15 12.77	14 50.78	14 19.16	13 50.43	13 23.91
	2.09	*2.09*	*2.10*	*2.11*	*2.12*	*2.15*	*2.17*	*2.21*
14.0	15 52.74	15 42.81	15 35.03	15 17.33	14 55.37	14 23.79	13 55.13	13 28.67
	2.42	*2.43*	*2.43*	*2.44*	*2.46*	*2.49*	*2.52*	*2.55*
16.0	15 57.91	15 47.99	15 40.22	15 22.54	15 00.62	14 29.09	14 00.50	13 34.12
	2.75	*2.75*	*2.76*	*2.77*	*2.79*	*2.82*	*2.85*	*2.89*
18.0	16 03.72	15 53.82	15 46.06	15 28.41	15 06.52	14 35.06	14 06.53	13 40.24
	3.07	*3.07*	*3.08*	*3.09*	*3.11*	*3.14*	*3.18*	*3.22*
20.0	16 10.16	16 00.27	15 52.52	15 34.90	15 13.06	14 41.66	14 13.22	13 47.01
	3.38	*3.38*	*3.39*	*3.40*	*3.42*	*3.46*	*3.50*	*3.55*
22.0	16 17.22	16 07.33	15 59.60	15 42.01	15 20.21	14 48.88	14 20.52	13 54.42
	3.68	*3.68*	*3.69*	*3.70*	*3.73*	*3.76*	*3.81*	*3.86*
24.0	16 24.86	16 14.99	16 07.27	15 49.72	15 27.96	14 56.71	14 28.43	14 02.43
	3.97	*3.97*	*3.98*	*4.00*	*4.02*	*4.06*	*4.10*	*4.16*
26.0	16 33.08	16 23.22	16 15.52	15 58.00	15 36.28	15 05.11	14 36.93	14 11.03
	4.25	*4.26*	*4.26*	*4.28*	*4.30*	*4.34*	*4.39*	*4.44*
28.0	16 41.85	16 32.00	16 24.31	16 06.83	15 45.17	15 14.07	14 45.98	14 20.19
	4.52	*4.53*	*4.53*	*4.55*	*4.58*	*4.62*	*4.66*	*4.72*
30.0	16 51.15	16 41.31	16 33.64	16 16.20	15 54.58	15 23.57	14 55.58	14 29.90
	4.78	*4.79*	*4.80*	*4.81*	*4.84*	*4.88*	*4.93*	*4.98*
32.0	17 00.96	16 51.14	16 43.49	16 26.08	16 04.51	15 33.58	15 05.68	14 40.12
	5.03	*5.04*	*5.05*	*5.06*	*5.09*	*5.13*	*5.18*	*5.23*
34.0	17 11.27	17 01.45	16 53.82	16 36.45	16 14.93	15 44.08	15 16.28	14 50.83
	5.27	*5.28*	*5.28*	*5.30*	*5.33*	*5.37*	*5.42*	*5.47*
36.0	17 22.04	17 12.24	17 04.62	16 47.29	16 25.82	15 55.05	15 27.34	15 02.00
	5.50	*5.51*	*5.51*	*5.53*	*5.56*	*5.60*	*5.65*	*5.70*
38.0	17 33.25	17 23.47	17 15.86	16 58.57	16 37.15	16 06.46	15 38.85	15 13.62
	5.72	*5.72*	*5.73*	*5.75*	*5.77*	*5.81*	*5.86*	*5.92*
40.0	17 44.89	17 35.12	17 27.53	17 10.28	16 48.91	16 18.30	15 50.78	15 25.66
	5.92	*5.93*	*5.94*	*5.96*	*5.98*	*6.02*	*6.07*	*6.12*
42.0	17 56.94	17 47.18	17 39.60	17 22.39	17 01.06	16 30.54	16 03.11	15 38.10
	6.12	*6.12*	*6.13*	*6.15*	*6.18*	*6.21*	*6.26*	*6.31*
44.0	18 09.37	17 59.62	17 52.06	17 34.88	17 13.60	16 43.15	16 15.81	15 50.90
	6.30	*6.31*	*6.32*	*6.34*	*6.36*	*6.40*	*6.44*	*6.49*
46.0	18 22.15	18 12.41	18 04.87	17 47.73	17 26.50	16 56.12	16 28.87	16 04.06
	6.48	*6.49*	*6.49*	*6.51*	*6.53*	*6.57*	*6.61*	*6.66*
48.0	18 35.28	18 25.55	18 18.03	18 00.91	17 39.73	17 09.42	16 42.26	16 17.55
	6.65	*6.65*	*6.66*	*6.68*	*6.70*	*6.73*	*6.77*	*6.82*
50.0	18 48.73	18 39.02	18 31.50	18 14.42	17 53.28	17 23.04	16 55.96	16 31.34
	6.80	*6.81*	*6.81*	*6.83*	*6.85*	*6.89*	*6.92*	*6.97*

Table A1. (*continued*)

ScS	Depth of source [km]							
Δ	0.	35.	70.	150.	250.	400.	550.	700.
	m s	m s	m s	m s	m s	m s	m s	m s
50.0	18 48.73 *6.80*	18 39.02 *6.81*	18 31.50 *6.81*	18 14.42 *6.83*	17 53.28 *6.85*	17 23.04 *6.89*	16 55.96 *6.92*	16 31.34 *6.97*
52.0	19 02.48 *6.95*	18 52.78 *6.95*	18 45.28 *6.96*	18 28.23 *6.97*	18 07.12 *6.99*	17 36.95 *7.03*	17 09.95 *7.07*	16 45.42 *7.11*
54.0	19 16.52 *7.08*	19 06.82 *7.09*	18 59.33 *7.09*	18 42.31 *7.11*	18 21.25 *7.13*	17 51.14 *7.16*	17 24.21 *7.20*	16 59.77 *7.24*
56.0	19 30.81 *7.21*	19 21.13 *7.22*	19 13.65 *7.22*	18 56.66 *7.24*	18 35.64 *7.26*	18 05.59 *7.28*	17 38.73 *7.32*	17 14.37 *7.36*
58.0	19 45.36 *7.33*	19 35.68 *7.34*	19 28.22 *7.34*	19 11.25 *7.35*	18 50.26 *7.37*	18 20.27 *7.40*	17 53.48 *7.43*	17 29.19 *7.47*
60.0	20 00.13 *7.44*	19 50.46 *7.45*	19 43.01 *7.45*	19 26.07 *7.46*	19 05.11 *7.48*	18 35.18 *7.51*	18 08.45 *7.54*	17 44.23 *7.57*
62.0	20 15.12 *7.54*	20 05.46 *7.55*	19 58.01 *7.55*	19 41.10 *7.56*	19 20.17 *7.58*	18 50.29 *7.60*	18 23.62 *7.63*	17 59.47 *7.66*
64.0	20 30.30 *7.64*	20 20.65 *7.64*	20 13.21 *7.65*	19 56.32 *7.66*	19 35.43 *7.67*	19 05.59 *7.69*	18 38.97 *7.72*	18 14.89 *7.75*
66.0	20 45.67 *7.72*	20 36.02 *7.73*	20 28.59 *7.73*	20 11.72 *7.74*	19 50.85 *7.76*	19 21.06 *7.78*	18 54.49 *7.80*	18 30.47 *7.83*
68.0	21 01.20 *7.80*	20 51.56 *7.81*	20 44.14 *7.81*	20 27.29 *7.82*	20 06.44 *7.83*	19 36.69 *7.85*	19 10.17 *7.88*	18 46.20 *7.90*
70.0	21 16.88 *7.88*	21 07.25 *7.88*	20 59.84 *7.88*	20 43.01 *7.89*	20 22.18 *7.90*	19 52.47 *7.92*	19 25.99 *7.94*	19 02.07 *7.97*
72.0	21 32.70 *7.94*	21 23.07 *7.95*	21 15.67 *7.95*	20 58.86 *7.96*	20 38.06 *7.97*	20 08.37 *7.98*	19 41.94 *8.00*	19 18.06 *8.02*
74.0	21 48.65 *8.00*	21 39.03 *8.01*	21 31.63 *8.01*	21 14.83 *8.02*	20 54.05 *8.02*	20 24.40 *8.04*	19 58.00 *8.06*	19 34.16 *8.08*
76.0	22 04.71 *8.06*	21 55.09 *8.06*	21 47.70 *8.06*	21 30.92 *8.07*	21 10.15 *8.08*	20 40.53 *8.09*	20 14.16 *8.10*	19 50.36 *8.12*
78.0	22 20.88 *8.10*	22 11.26 *8.11*	22 03.88 *8.11*	21 47.10 *8.12*	21 26.35 *8.12*	20 56.76 *8.14*	20 30.42 *8.15*	20 06.64 *8.16*
80.0	22 37.13 *8.15*	22 27.52 *8.15*	22 20.14 *8.15*	22 03.38 *8.16*	21 42.64 *8.16*	21 13.07 *8.17*	20 46.75 *8.19*	20 23.01 *8.20*
82.0	22 53.47 *8.19*	22 43.86 *8.19*	22 36.48 *8.19*	22 19.73 *8.19*	21 59.00 *8.20*	21 29.45 *8.21*	21 03.16 *8.22*	20 39.43 *8.23*
84.0	23 09.87 *8.22*	23 00.26 *8.22*	22 52.89 *8.22*	22 36.15 *8.22*	22 15.43 *8.23*	21 45.89 *8.24*	21 19.62 *8.24*	20 55.92 *8.26*
86.0	23 26.33 *8.24*	23 16.73 *8.25*	23 09.36 *8.25*	22 52.62 *8.25*	22 31.92 *8.26*	22 02.39 *8.26*	21 36.13 *8.27*	21 12.45 *8.28*
88.0	23 42.85 *8.27*	23 33.24 *8.27*	23 25.88 *8.27*	23 09.14 *8.27*	22 48.45 *8.28*	22 18.94 *8.28*	21 52.69 *8.29*	21 29.02 *8.29*
90.0	23 59.40 *8.29*	23 49.80 *8.29*	23 42.44 *8.29*	23 25.71 *8.29*	23 05.02 *8.29*	22 35.51 *8.30*	22 09.28 *8.30*	21 45.62 *8.31*
92.0	24 15.99 *8.30*	24 06.39 *8.30*	23 59.03 *8.30*	23 42.30 *8.30*	23 21.62 *8.31*	22 52.12 *8.31*	22 25.89 *8.31*	22 02.24 *8.31*
94.0	24 32.60 *8.31*	24 23.00 *8.31*	24 15.64 *8.31*	23 58.92 *8.31*	23 38.24 *8.31*	23 08.75 *8.32*	22 42.53 *8.32*	22 18.88 *8.32*
96.0	24 49.23 *8.32*	24 39.64 *8.32*	24 32.28 *8.32*	24 15.56 *8.32*	23 54.88 *8.32*	23 25.39 *8.32*	22 59.17 *8.32*	
98.0	25 05.88 *8.32*	24 56.28 *8.32*	24 48.92 *8.32*	24 32.20 *8.32*	24 11.52 *8.32*			

Table A1. (*continued*)

SKSac	Depth of source [km]							
Δ	0.	35.	70.	150.	250.	400.	550.	700.
	m s	m s	m s	m s	m s	m s	m s	m s
64.0	20 30.27	20 20.62	20 13.18	19 56.27	19 35.35	19 05.46	18 38.77	18 14.57
	7.59	*7.59*	*7.59*	*7.59*	*7.59*	*7.58*	*7.58*	*7.57*
66.0	20 45.44	20 35.78	20 28.34	20 11.43	19 50.51	19 20.61	18 53.91	18 29.70
	7.58	*7.58*	*7.58*	*7.58*	*7.57*	*7.57*	*7.56*	*7.55*
68.0	21 00.58	20 50.92	20 43.48	20 26.56	20 05.63	19 35.72	19 09.00	18 44.76
	7.56	*7.56*	*7.56*	*7.55*	*7.55*	*7.54*	*7.53*	*7.51*
70.0	21 15.67	21 06.01	20 58.56	20 41.64	20 20.69	19 50.76	19 24.01	18 59.74
	7.53	*7.53*	*7.52*	*7.52*	*7.51*	*7.50*	*7.48*	*7.46*
72.0	21 30.67	21 21.01	21 13.55	20 56.62	20 35.66	20 05.70	19 38.90	19 14.58
	7.47	*7.47*	*7.47*	*7.46*	*7.45*	*7.43*	*7.41*	*7.37*
74.0	21 45.55	21 35.88	21 28.42	21 11.46	20 50.47	20 20.47	19 53.62	19 29.21
	7.40	*7.39*	*7.39*	*7.38*	*7.36*	*7.34*	*7.30*	*7.26*
76.0	22 00.24	21 50.56	21 43.09	21 26.11	21 05.08	20 35.01	20 08.09	19 43.59
	7.29	*7.28*	*7.28*	*7.26*	*7.24*	*7.21*	*7.16*	*7.11*
78.0	22 14.67	22 04.98	21 57.50	21 40.48	21 19.41	20 49.27	20 22.25	19 57.63
	7.14	*7.14*	*7.13*	*7.11*	*7.08*	*7.04*	*6.99*	*6.93*
80.0	22 28.78	22 19.07	22 11.57	21 54.52	21 33.39	21 03.16	20 36.03	20 11.29
	6.96	*6.95*	*6.94*	*6.92*	*6.89*	*6.85*	*6.79*	*6.73*
82.0	22 42.50	22 32.78	22 25.26	22 08.15	21 46.97	21 16.64	20 49.40	20 24.54
	6.75	*6.75*	*6.74*	*6.71*	*6.68*	*6.64*	*6.58*	*6.51*
84.0	22 55.78	22 46.05	22 38.51	22 21.36	22 00.12	21 29.69	21 02.34	20 37.35
	6.53	*6.53*	*6.51*	*6.49*	*6.46*	*6.42*	*6.36*	*6.30*
86.0	23 08.62	22 58.87	22 51.31	22 34.12	22 12.82	21 42.31	21 14.85	20 49.74
	6.31	*6.30*	*6.29*	*6.27*	*6.24*	*6.20*	*6.15*	*6.09*
88.0	23 21.02	23 11.25	23 03.68	22 46.44	22 25.09	21 54.49	21 26.93	21 01.71
	6.09	*6.08*	*6.07*	*6.05*	*6.03*	*5.98*	*5.94*	*5.88*
90.0	23 32.98	23 23.20	23 15.61	22 58.34	22 36.93	22 06.25	21 38.60	21 13.27
	5.87	*5.87*	*5.86*	*5.84*	*5.82*	*5.78*	*5.73*	*5.68*
92.0	23 44.52	23 34.73	23 27.12	23 09.81	22 48.36	22 17.60	21 49.87	21 24.44
	5.67	*5.66*	*5.65*	*5.64*	*5.61*	*5.58*	*5.54*	*5.49*
94.0	23 55.65	23 45.85	23 38.23	23 20.89	22 59.39	22 28.56	22 00.75	21 35.24
	5.47	*5.46*	*5.46*	*5.44*	*5.42*	*5.39*	*5.35*	*5.30*
96.0	24 06.40	23 56.59	23 48.95	23 31.58	23 10.04	22 39.15	22 11.26	21 45.67
	5.28	*5.27*	*5.27*	*5.25*	*5.23*	*5.20*	*5.17*	*5.13*
98.0	24 16.78	24 06.95	23 59.30	23 41.90	23 20.33	22 49.38	22 21.42	21 55.75
	5.10	*5.09*	*5.09*	*5.07*	*5.05*	*5.03*	*4.99*	*4.96*
100.0	24 26.79	24 16.96	24 09.30	23 51.87	23 30.27	22 59.26	22 31.24	22 05.50
	4.92	*4.92*	*4.91*	*4.90*	*4.88*	*4.86*	*4.82*	*4.79*
102.0	24 36.46	24 26.63	24 18.95	24 01.50	23 39.86	23 08.80	22 40.72	22 14.92
	4.75	*4.75*	*4.74*	*4.73*	*4.72*	*4.69*	*4.66*	*4.63*
104.0	24 45.80	24 35.96	24 28.28	24 10.80	23 49.13	23 18.02	22 49.89	22 24.02
	4.59	*4.59*	*4.58*	*4.57*	*4.55*	*4.53*	*4.51*	*4.47*
106.0	24 54.82	24 44.97	24 37.28	24 19.78	23 58.09	23 26.93	22 58.75	22 32.82
	4.43	*4.43*	*4.42*	*4.41*	*4.40*	*4.38*	*4.35*	*4.33*
108.0	25 03.54	24 53.68	24 45.97	24 28.46	24 06.74	23 35.54	23 07.31	22 41.33
	4.28	*4.28*	*4.27*	*4.26*	*4.25*	*4.23*	*4.21*	*4.18*
110.0	25 11.95	25 02.08	24 54.37	24 36.84	24 15.09	23 43.86	23 15.58	22 49.55
	4.13	*4.13*	*4.13*	*4.12*	*4.11*	*4.09*	*4.07*	*4.04*
112.0	25 20.08	25 10.20	25 02.49	24 44.93	24 23.17	23 51.90	23 23.58	22 57.50
	3.99	*3.99*	*3.99*	*3.98*	*3.97*	*3.95*	*3.93*	*3.91*
114.0	25 27.92	25 18.05	25 10.32	24 52.75	24 30.96	23 59.66	23 31.30	23 05.18
	3.86	*3.85*	*3.85*	*3.84*	*3.83*	*3.81*	*3.79*	*3.77*

Table A1. (*continued*)

SKSac	Depth of source [km]							
Δ	0.	35.	70.	150.	250.	400.	550.	700.
	m s	m s	m s	m s	m s	m s	m s	m s
114.0	25 27.92	25 18.05	25 10.32	24 52.75	24 30.96	23 59.66	23 31.30	23 05.18
	3.86	*3.85*	*3.85*	*3.84*	*3.83*	*3.81*	*3.79*	*3.77*
116.0	25 35.50	25 25.61	25 17.88	25 00.30	24 38.49	24 07.15	23 38.76	23 12.60
	3.72	*3.72*	*3.71*	*3.71*	*3.70*	*3.68*	*3.66*	*3.64*
118.0	25 42.80	25 32.92	25 25.18	25 07.58	24 45.75	24 14.39	23 45.96	23 19.76
	3.59	*3.59*	*3.58*	*3.58*	*3.57*	*3.55*	*3.54*	*3.52*
120.0	25 49.85	25 39.96	25 32.22	25 14.60	24 52.76	24 21.36	23 52.90	23 26.66
	3.46	*3.46*	*3.45*	*3.45*	*3.44*	*3.43*	*3.41*	*3.39*
122.0	25 56.65	25 46.75	25 39.00	25 21.38	24 59.52	24 28.09	23 59.60	23 33.33
	3.34	*3.33*	*3.33*	*3.32*	*3.32*	*3.30*	*3.29*	*3.27*
124.0	26 03.19	25 53.29	25 45.54	25 27.90	25 06.03	24 34.58	24 06.06	23 39.75
	3.21	*3.21*	*3.21*	*3.20*	*3.19*	*3.18*	*3.17*	*3.15*
126.0	26 09.50	25 59.59	25 51.84	25 34.19	25 12.29	24 40.82	24 12.27	23 45.94
	3.09	*3.09*	*3.09*	*3.08*	*3.08*	*3.06*	*3.05*	*3.04*
128.0	26 15.56	26 05.66	25 57.90	25 40.23	25 18.33	24 46.83	24 18.26	23 51.89
	2.97	*2.97*	*2.97*	*2.96*	*2.96*	*2.95*	*2.93*	*2.92*
130.0	26 21.40	26 11.49	26 03.72	25 46.05	25 24.13	24 52.61	24 24.02	23 57.62
	2.86	*2.86*	*2.86*	*2.85*	*2.84*	*2.83*	*2.82*	*2.81*
132.0	26 27.00	26 17.09	26 09.32	25 51.63	25 29.70	24 58.17	24 29.55	24 03.13
	2.74	*2.74*	*2.74*	*2.74*	*2.73*	*2.72*	*2.71*	*2.70*
134.0	26 32.38	26 22.46	26 14.69	25 57.00	25 35.05	25 03.50	24 34.86	24 08.41
	2.63	*2.63*	*2.63*	*2.62*	*2.62*	*2.61*	*2.60*	*2.59*
136.0	26 37.53	26 27.61	26 19.83	26 02.14	25 40.18	25 08.61	24 39.95	24 13.48
	2.52	*2.52*	*2.52*	*2.52*	*2.51*	*2.50*	*2.49*	*2.48*
138.0	26 42.47	26 32.55	26 24.76	26 07.06	25 45.09	25 13.50	24 44.82	24 18.33
	2.41	*2.41*	*2.41*	*2.41*	*2.40*	*2.39*	*2.38*	*2.37*
140.0	26 47.19	26 37.26	26 29.48	26 11.76	25 49.79	25 18.18	24 49.48	24 22.97
	2.31	*2.30*	*2.30*	*2.30*	*2.29*	*2.29*	*2.28*	*2.27*
142.0	26 51.69	26 41.76	26 33.98	26 16.25	25 54.27	25 22.65	24 53.93	24 27.40
	2.20	*2.20*	*2.20*	*2.19*	*2.19*	*2.18*	*2.17*	*2.16*
144.0	26 55.98	26 46.05	26 38.26	26 20.53	25 58.54	25 26.90	24 53.93	24 27.40
	2.09	*2.09*	*2.09*	*2.09*	*2.08*	*2.07*	*2.17*	*2.16*

Table A1. (*continued*)

SKSdf	Depth of source [km]							
Δ	0.	35.	70.	150.	250.	400.	550.	700.
	m s	m s	m s	m s	m s	m s	m s	m s
104.0	25 35.15	25 25.22	25 17.42	24 59.68	24 37.68	24 06.02	23 37.26	23 10.69
	1.91	*1.91*	*1.91*	*1.91*	*1.91*	*1.91*	*1.91*	*1.91*
106.0	25 38.98	25 29.05	25 21.25	25 03.51	24 41.51	24 09.85	23 41.09	23 14.52
	1.91	*1.91*	*1.91*	*1.91*	*1.91*	*1.91*	*1.91*	*1.91*
108.0	25 42.81	25 32.88	25 25.08	25 07.34	24 45.34	24 13.68	23 44.92	23 18.34
	1.91	*1.91*	*1.91*	*1.91*	*1.91*	*1.91*	*1.91*	*1.91*
110.0	25 46.63	25 36.70	25 28.91	25 11.16	24 49.16	24 17.50	23 48.74	23 22.17
	1.91	*1.91*	*1.91*	*1.91*	*1.91*	*1.91*	*1.91*	*1.91*
112.0	25 50.46	25 40.52	25 32.73	25 14.99	24 52.98	24 21.32	23 52.56	23 25.99
	1.91	*1.91*	*1.91*	*1.91*	*1.91*	*1.91*	*1.91*	*1.91*
114.0	25 54.27	25 44.33	25 36.54	25 18.80	24 56.79	24 25.13	23 56.37	23 29.80
	1.90	*1.90*	*1.90*	*1.90*	*1.90*	*1.90*	*1.90*	*1.90*
116.0	25 58.07	25 48.14	25 40.34	25 22.60	25 00.60	24 28.94	24 00.18	23 33.60
	1.90	*1.90*	*1.90*	*1.90*	*1.90*	*1.90*	*1.90*	*1.90*
118.0	26 01.87	25 51.93	25 44.14	25 26.39	25 04.39	24 32.73	24 03.97	23 37.39
	1.89	*1.89*	*1.89*	*1.89*	*1.89*	*1.89*	*1.89*	*1.89*
120.0	26 05.64	25 55.71	25 47.91	25 30.17	25 08.16	24 36.50	24 07.74	23 41.16
	1.88	*1.88*	*1.88*	*1.88*	*1.88*	*1.88*	*1.88*	*1.88*
122.0	26 09.40	25 59.47	25 51.67	25 33.93	25 11.92	24 40.26	24 11.49	23 44.91
	1.87	*1.87*	*1.87*	*1.87*	*1.87*	*1.87*	*1.87*	*1.87*
124.0	26 13.14	26 03.20	25 55.41	25 37.66	25 15.65	24 43.99	24 15.22	23 48.64
	1.86	*1.86*	*1.86*	*1.86*	*1.86*	*1.86*	*1.86*	*1.86*
126.0	26 16.84	26 06.91	25 59.11	25 41.37	25 19.36	24 47.69	24 18.92	23 52.34
	1.85	*1.85*	*1.85*	*1.85*	*1.84*	*1.84*	*1.84*	*1.84*
128.0	26 20.52	26 10.58	26 02.78	25 45.04	25 23.03	24 51.36	24 22.59	23 56.00
	1.83	*1.83*	*1.83*	*1.83*	*1.83*	*1.82*	*1.82*	*1.82*
130.0	26 24.15	26 14.21	26 06.41	25 48.67	25 26.65	24 54.98	24 26.21	23 59.62
	1.80	*1.80*	*1.80*	*1.80*	*1.80*	*1.80*	*1.80*	*1.80*
132.0	26 27.73	26 17.79	26 09.99	25 52.25	25 30.23	24 58.56	24 29.78	24 03.18
	1.78	*1.78*	*1.78*	*1.78*	*1.77*	*1.77*	*1.77*	*1.77*
134.0	26 31.25	26 21.32	26 13.52	25 55.77	25 33.75	25 02.07	24 33.29	24 06.69
	1.75	*1.75*	*1.75*	*1.74*	*1.74*	*1.74*	*1.74*	*1.74*
136.0	26 34.71	26 24.77	26 16.97	25 59.22	25 37.20	25 05.52	24 36.73	24 10.12
	1.71	*1.71*	*1.71*	*1.71*	*1.71*	*1.70*	*1.70*	*1.70*
138.0	26 38.08	26 28.15	26 20.34	26 02.59	25 40.57	25 08.88	24 40.09	24 13.48
	1.67	*1.67*	*1.67*	*1.66*	*1.66*	*1.66*	*1.66*	*1.65*
140.0	26 41.37	26 31.43	26 23.63	26 05.87	25 43.85	25 12.16	24 43.36	24 16.74
	1.62	*1.62*	*1.62*	*1.62*	*1.62*	*1.61*	*1.61*	*1.61*
142.0	26 44.56	26 34.62	26 26.81	26 09.06	25 47.03	25 15.33	24 46.53	24 19.90
	1.57	*1.57*	*1.57*	*1.56*	*1.56*	*1.56*	*1.56*	*1.55*
144.0	26 47.63	26 37.69	26 29.89	26 12.13	25 50.09	25 18.39	24 49.58	24 22.95
	1.51	*1.51*	*1.51*	*1.51*	*1.50*	*1.50*	*1.50*	*1.49*
146.0	26 50.59	26 40.65	26 32.84	26 15.08	25 53.04	25 21.33	24 52.52	24 25.87
	1.45	*1.45*	*1.45*	*1.44*	*1.44*	*1.44*	*1.43*	*1.43*
148.0	26 53.41	26 43.47	26 35.66	26 17.90	25 55.86	25 24.14	24 55.32	24 28.67
	1.38	*1.38*	*1.38*	*1.38*	*1.37*	*1.37*	*1.37*	*1.36*
150.0	26 56.10	26 46.15	26 38.35	26 20.58	25 58.53	25 26.81	24 57.98	24 31.32
	1.31	*1.31*	*1.31*	*1.30*	*1.30*	*1.30*	*1.30*	*1.29*
152.0	26 58.64	26 48.69	26 40.89	26 23.11	26 01.07	25 29.34	25 00.50	24 33.84
	1.23	*1.23*	*1.23*	*1.23*	*1.23*	*1.23*	*1.22*	*1.22*
154.0	27 01.03	26 51.08	26 43.27	26 25.50	26 03.45	25 31.71	25 02.87	24 36.19
	1.15	*1.15*	*1.15*	*1.15*	*1.15*	*1.15*	*1.14*	*1.14*

Table A1. (*continued*)

SKSdf	Depth of source [km]							
Δ	0.	35.	70.	150.	250.	400.	550.	700.
	m s	m s	m s	m s	m s	m s	m s	m s
154.0	27 01.03	26 51.08	26 43.27	26 25.50	26 03.45	25 31.71	25 02.87	24 36.19
	1.15	*1.15*	*1.15*	*1.15*	*1.15*	*1.15*	*1.14*	*1.14*
156.0	27 03.26	26 53.31	26 45.50	26 27.72	26 05.67	25 33.93	25 05.08	24 38.40
	1.07	*1.07*	*1.07*	*1.07*	*1.07*	*1.07*	*1.06*	*1.06*
158.0	27 05.32	26 55.38	26 47.56	26 29.78	26 07.73	25 35.98	25 07.12	24 40.44
	0.99	*0.99*	*0.99*	*0.99*	*0.99*	*0.99*	*0.98*	*0.98*
160.0	27 07.22	26 57.27	26 49.46	26 31.68	26 09.62	25 37.87	25 09.00	24 42.31
	0.91	*0.91*	*0.91*	*0.90*	*0.90*	*0.90*	*0.90*	*0.89*
162.0	27 08.95	26 59.00	26 51.19	26 33.40	26 11.34	25 39.58	25 10.72	24 44.01
	0.82	*0.82*	*0.82*	*0.82*	*0.82*	*0.81*	*0.81*	*0.81*
164.0	27 10.50	27 00.55	26 52.74	26 34.95	26 12.88	25 41.13	25 12.25	24 45.55
	0.73	*0.73*	*0.73*	*0.73*	*0.73*	*0.73*	*0.73*	*0.72*
166.0	27 11.88	27 01.93	26 54.11	26 36.32	26 14.25	25 42.49	25 13.61	24 46.90
	0.64	*0.64*	*0.64*	*0.64*	*0.64*	*0.64*	*0.64*	*0.63*
168.0	27 13.07	27 03.12	26 55.31	26 37.52	26 15.45	25 43.68	25 14.80	24 48.08
	0.55	*0.55*	*0.55*	*0.55*	*0.55*	*0.55*	*0.55*	*0.55*
170.0	27 14.09	27 04.14	26 56.32	26 38.53	26 16.46	25 44.69	25 15.80	24 49.08
	0.46	*0.46*	*0.46*	*0.46*	*0.46*	*0.46*	*0.46*	*0.46*
172.0	27 14.92	27 04.97	26 57.15	26 39.36	26 17.29	25 45.52	25 16.63	24 49.90
	0.37	*0.37*	*0.37*	*0.37*	*0.37*	*0.37*	*0.37*	*0.37*
174.0	27 15.57	27 05.62	26 57.80	26 40.01	26 17.93	25 46.16	25 17.27	24 50.54
	0.28	*0.28*	*0.28*	*0.28*	*0.28*	*0.28*	*0.28*	*0.27*
176.0	27 16.04	27 06.08	26 58.26	26 40.47	26 18.39	25 46.62	25 17.73	24 51.00
	0.19	*0.19*	*0.19*	*0.19*	*0.19*	*0.18*	*0.18*	*0.18*
178.0	27 16.31	27 06.36	26 58.54	26 40.75	26 18.67	25 46.90	25 18.00	24 51.28
	0.09	*0.09*	*0.09*	*0.09*	*0.09*	*0.09*	*0.09*	*0.09*
180.0	27 16.41	27 06.45	26 58.64	26 40.84	26 18.76	25 46.99	25 18.10	24 51.37
	0.00	*0.00*	*0.00*	*0.00*	*0.00*	*0.00*	*0.00*	*0.00*

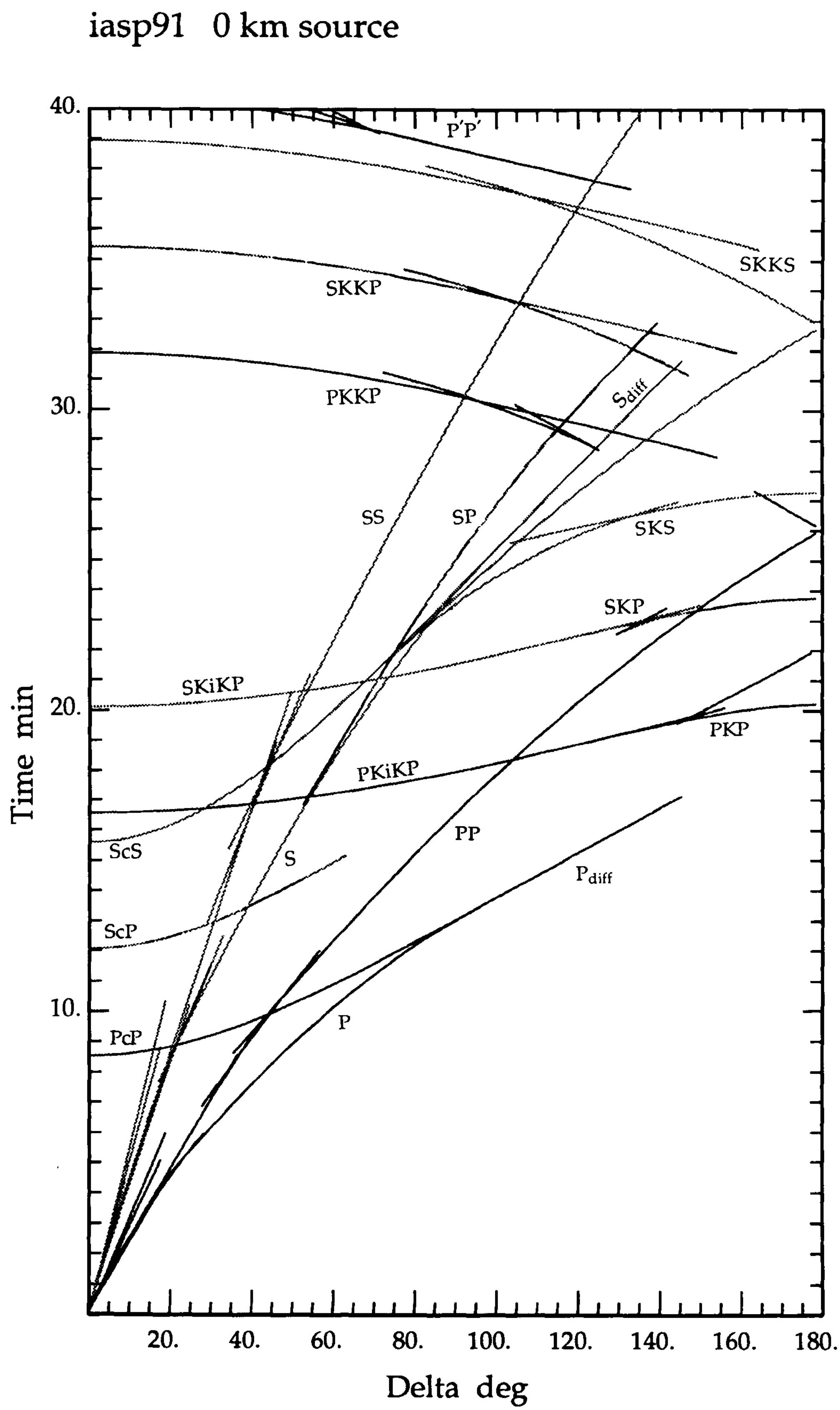

Figure A1. Traveltime curves for the *iasp91* model for surface focus.

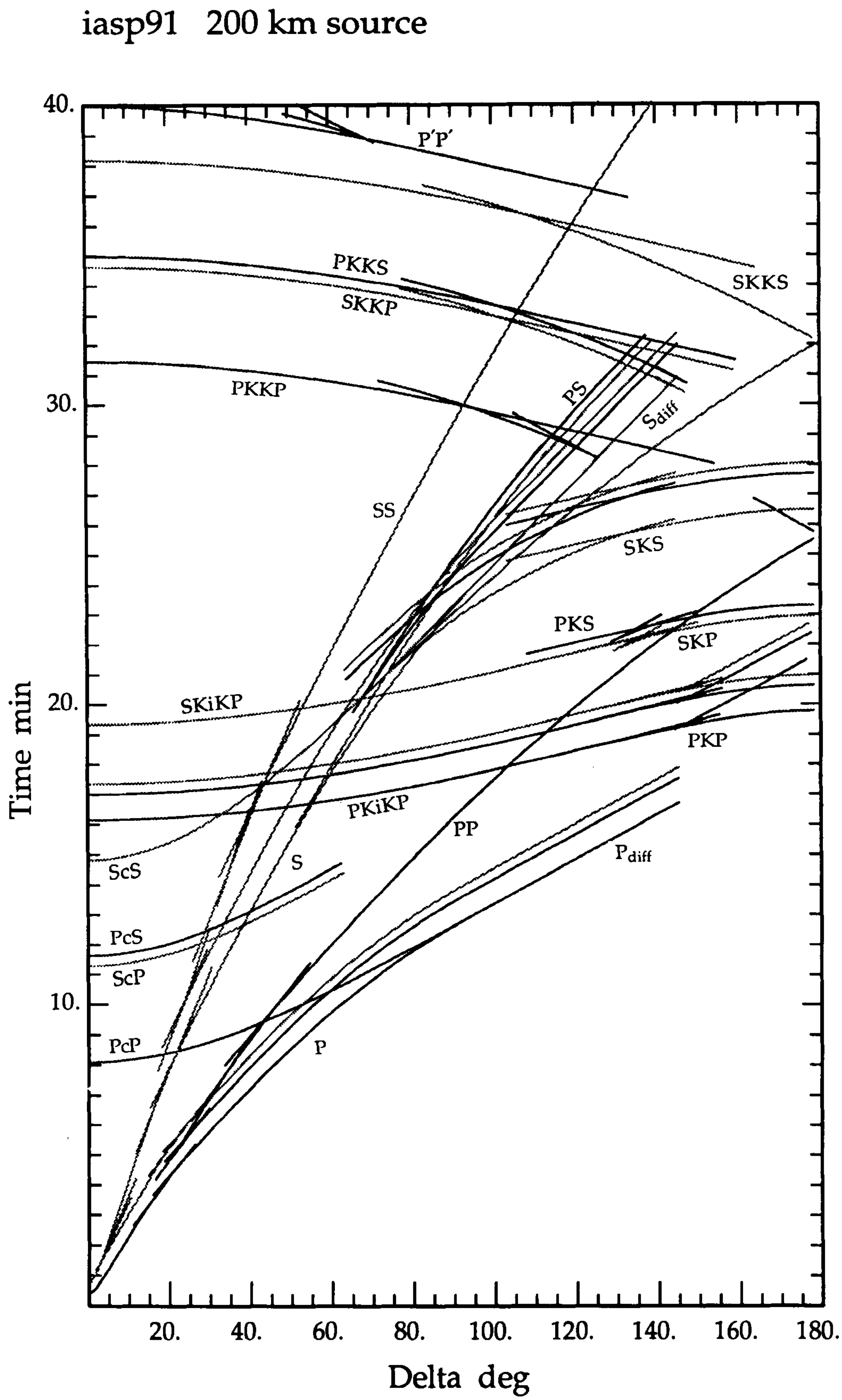

Figure A2. Traveltime curves for the *iasp91* model for 200 km focal depth.

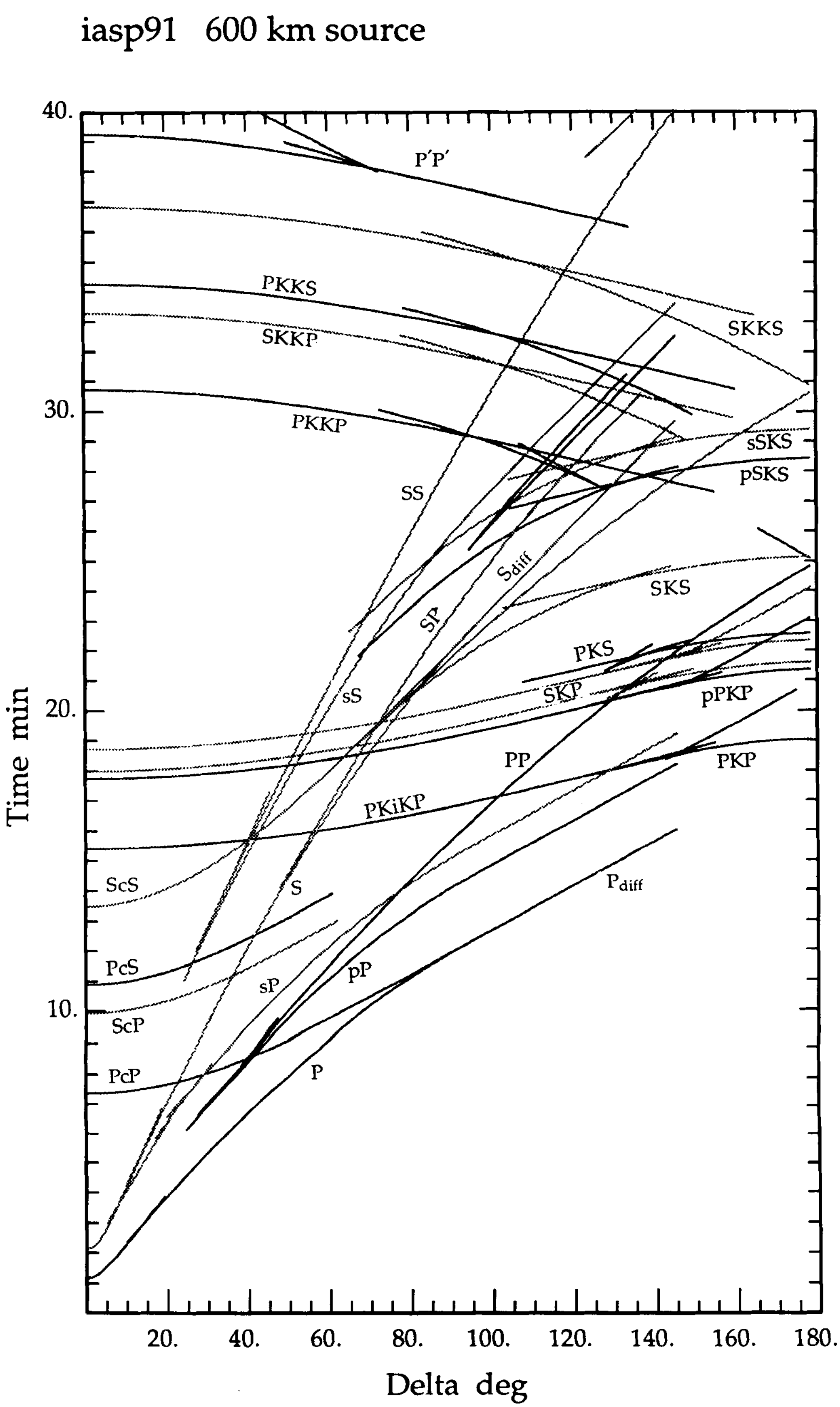

Figure A3. Traveltime curves for the *iasp91* model for 600 km focal depth.

APPENDIX B

Hypocentral parameters for test events

The following table summarizes the hypocentral information supplied by contributors for the 104 test events. The 83 earthquakes are shown first and then the 21 explosions. For those explosions marked with an asterisk the location has been derived as if the event were an earthquake. In the other cases the hypocentral information is not derived from seismological data. For the explosions in Eastern Kazakh, the hypocentral parameters were taken from data recently published in the Soviet Union (Bocharov, Zelentsov & Mikhailov 1989—translated in Vergino 1989)

Table B1. Hypocentral information for test events.

Earthquakes:

Date	Time	Lat.	Long.	Depth	mb	
1973 04 26	20 26 30.6	19.903	-155.13	48	5.9	Kalapana (Hawaii,USA)
1983 11 16	16 12 58.57	19.419	-155.453	12.5	6.3	Kaoiki (Hawaii,USA)
1989 06 26	03 27 03.90	19.362	-155.083	9	5.8	(Hawaii,USA)
1984 05 06	19 54 49.00	51.364	-176.604	37.0	5.7	Adak (Alaska,USA)
1988 02 07	08 46 58.59	60.296	-152.973	137.7	5.6	Redoubt (Alaska,USA)
1984 08 14	01 02 09.31	61.824	-148.975	18.7	5.7	Sutton (Alaska,USA)
1983 09 07	10 22 05.00	60.979	-147.320	30.0	6.2	Columbia Bay (Alaska,USA)
1983 06 28	03 25 17.15	60.180	-141.250	13.4	6.0	St. Elias (Alaska,USA)
1985 12 23	05 16 02.4	62.187	-124.242	6.0	6.4	Nahanni (Canada)
1988 11 25	23 46 04.5	48.117	-71.183	28.9	5.9	Saguenay (Canada)
1982 01 09	12 53 51.7	47.0	-66.6	6	5.7	Miramichi (Canada)
1976 05 16	08 35 15.09	48.794	-123.340	62.0	5.2	Gulf Islands (Canada)
1981 02 14	06 09 27.18	46.351	-122.238	8.5	5.1	Elk Lake (WA,USA)
1987 07 31	23 56 57.83	40.418	-124.406	17.7	5.6	Eureka (CA,USA)
1986 03 31	11 55 39.94	37.468	-121.694	6.4	5.4	Mt. Lewis (CA,USA)
1984 04 24	21 15 18.74	37.311	-121.679	8.8	5.6	Morgan Hill (CA,USA)
1979 08 06	17 05 22.39	37.114	-121.496	7.5	5.3	Coyote Lake (CA,USA)
1986 01 26	19 20 51.08	36.809	-121.268	6.4	5.2	Hollister (CA,USA)
1983 05 02	23 42 38.15	36.232	-120.310	10.0	6.1	Coalinga (CA,USA)
1983 07 22	02 39 54.07	36.240	-120.409	7.3	6.0	Coalinga (CA,USA)
1986 07 21	14 42 26.03	37.533	-118.446	9.7	6.0	Chalfont Valley (CA,USA)
1987 10 01	14 42 19.47	34.049	-118.081	14.4	5.8	Whittier (CA,USA)
1986 07 08	09 20 44.44	33.999	-116.610	11.7	5.8	Palm Springs (CA,USA)
1987 11 24	13 15 56.54	33.015	-115.849	1.9	6.0	Superstition Hills (CA,USA)
1983 10 28	14 06 06.79	43.968	-113.899	16.0	6.2	Borah Peak (ID,USA)
1983 10 07	10 18 46.32	43.946	-74.252	7.8	5.1	Goodnow (NY, USA)
1980 07 27	18 52 21.52	38.195	-83.937	16.6	5.1	Sharpsburg (KY,USA)
1986 10 10	17 49 24.71	13.650	-89.200	10.9	5.0	El Salvador
1987 03 21	12 08 57.86	8.725	-83.582	35.1	5.3	Costa Rica
1984 02 11	13 57 44.6	12.128	-59.970	60.0	5.3	Eastern Caribbean
1985 03 16	14 53 59.9	17.066	-62.379	15.8	6.1	Eastern Caribbean
1985 03 17	10 41 36.72	-32.735	-71.778	23.2	5.8	Chile
1988 03 25	17 20 54.35	-31.410	-67.977	24.4	5.3	Argentina
1987 05 25	11 31 54.70	63.909	-19.779	11.3	5.7	Vatnafjoll (Iceland)
1985 07 13	18 54 14.89	25.771	-45.053	6.4	5.0	North Atlantic Ridge
1989 01 23	14 06 28.91	61.933	4.432	26.2	5.5	Norway
1981 02 25	02 35 52.20	38.140	23.080	6.0	5.7	Greece
1982 01 18	19 27 24.50	39.840	24.470	15.0	5.8	Greece
1983 01 17	12 41 30.70	37.960	20.230	6.0	7.0	Greece
1984 10 25	14 38 28.30	40.090	21.610	4.0	5.2	Greece
1989 01 25	10 14 35.2	-28.004	26.752	1.7	5.5	Welkom (South Africa)
1983 10 30	04 12 26.9	40.31	42.10	15.0	6.0	Turkey
1986 05 13	08 44 00.8	41.45	43.70	10.0	5.5	Turkey-USSR
1984 03 04	10 01 33.6	43.08	45.48	25.0	5.2	Caucasus (USSR)
1985 10 29	13 13 40.2	36.78	54.80	20.0	6.0	Iran
1983 03 14	12 12 44.4	39.30	54.60	10.0	5.2	Turkmen (USSR)
1984 02 22	05 44 37.3	39.34	54.07	15.0	5.9	Turkmen (USSR)
1984 03 19	20 28 39.0	40.38	63.36	15.0	6.4	Uzbek (USSR)
1986 03 25	23 49 31.5	40.37	63.65	15.0	5.2	Uzbek (USSR)
1984 10 26	20 22 19.7	39.25	71.26	15.0	5.9	Tajik (USSR)
1985 10 13	15 59 52.0	40.30	69.80	10.0	5.8	Tajik (USSR)
1977 12 25	16 18 51.36	38.967	70.601	2.9	5.0	Garm (USSR)
1986 04 26	07 35 14.88	32.212	76.281	13.4	5.5	India
1985 08 23	12 41 56.8	39.37	75.44	20.0	6.2	Xinjiang (China)
1975 02 04	11 36 05.93	40.567	122.764	6.6	7.3	Haicheng (China)
1982 03 21	02 32 06.00	42.156	142.531	27.4	6.3	Urakawa-Oki (Japan)
1982 03 21	10 22 35.25	42.228	142.600	24.3	5.7	Urakawa-Oki (Japan)
1983 10 30	16 51 55.94	35.420	133.920	10.6	5.4	Tottori (Japan)
1983 07 01	22 03 42.20	36.893	141.190	43.4	5.5	Tohuku (Japan)
1987 01 09	06 14 45.82	39.832	141.764	74.6	6.4	Tohuku (Japan)
1983 02 27	12 14 21.6	35.993	140.105	67.0	5.7	Kanto-Tokai (Japan)
1983 08 08	03 47 58.6	35.536	139.046	18.1	5.8	Kanto-Tokai (Japan)
1984 04 06	01 09 03.8	35.123	138.601	191.4	5.1	Kanto-Tokai (Japan)
1984 09 13	23 48 49.1	35.807	137.554	1.1	6.0	Kanto-Tokai (Japan)
1985 10 04	12 25 52.3	35.910	140.112	71.6	5.7	Kanto-Tokai (Japan)
1986 11 22	00 41 44.5	34.616	139.446	2.1	5.8	Kanto-Tokai (Japan)
1987 12 17	02 08 17.3	35.372	140.519	47.3	6.0	Kanto-Tokai (Japan)
1988 03 17	20 34 30.1	35.668	139.626	90.5	5.4	Kanto-Tokai (Japan)
1989 02 19	12 27 10.5	36.049	139.905	45.4	5.5	Kanto-Tokai (Japan)
1989 03 06	14 39 44.7	35.706	140.666	51.5	5.9	Kanto-Tokai (Japan)
1983 03 17	07 11 26.7	51.55	142.41	20.0	5.6	Sakhalin Island (USSR)
1983 03 10	00 27 48.9	43.82	147.42	40.0	6.1	Kuril Islands (USSR)
1984 01 04	22 40 40.7	45.55	151.39	35.0	6.0	Kuril Islands (USSR)
1983 01 05	02 01 01.0	54.73	162.92	20.0	5.6	Kamchatka (USSR)
1984 11 01	18 43 39.4	55.23	163.72	20.0	5.8	Kamchatka (USSR)

Table B1. (*continued*)

Date	Time	Lat.	Long.	Depth	mb	Region
1984 12 28	10 37 50.5	56.29	163.49	13.0	7.5	Kamchatka (USSR)
1986 05 02	10 30 02.9	55.07	163.71	20.0	5.9	Kamchatka (USSR)
1985 09 10	01 26 04.8	60.50	168.86	15.0	5.6	Siberia (USSR)
1986 05 20	05 25 49.58	24.082	121.592	15.8	6.1	Taiwan
1968 10 14	02 58 50.3	-31.6	117.0	5	6.8	Meckering (Australia)
1988 01 22	00 35 59.5	-19.817	133.878	6.5	6.1	Tennant Creek (Australia)
1986 12 13	18 31 50.86	-18.109	167.625	2.4	5.4	Vanuatu Islands
1984 06 24	13 29 40.2	-43.59	170.64	9	5.6	Macaulay (New Zealand)

Explosions:

Date	Time	Lat.	Long.	Depth	mb	
1958 06 28	19 30 00.1	11.608	162.108	0.0		OAK (Eniwetok,USA)
1954 02 28	18 45 00.00	11.691	165.274	0.0		CASTLE BRAVO (Bikini,USA)
1954 05 04	18 10 00.10	11.666	165.387	0.0		CASTLE YANKEE (Bikini,USA)
1971 11 06	22 00 00.06	51.472	179.107	1.7	6.5	CANNIKIN (Alaska,USA)
1968 01 19	18 15 00.1	38.634	-116.215	0.0	6.3	FAULTLESS (NV,USA)
1968 04 26	15 00 00.10	37.295	-116.456	0.0	6.3	BOXCAR (NV,USA)
1988 07 07	15 05 30.07	37.252	-116.377	0.0	5.6	ALAMO (NV,USA)
1963 09 13	17 00 00.10	37.060	-116.022	0.0	5.8	BILBY (NV,USA)
1967 05 20	15 00 00.20	37.130	-116.064	0.0	5.9	COMMODORE (NV,USA)
1969 09 10	21 00 00.10	39.406	-107.948	0.1	5.3	RULISON (CO,USA)
1973 05 17	16 00 00.00	39.793	-108.366	0.0	5.4	RIO BLANCO (CO,USA)
1967 12 10	19 30 00.10	36.678	-107.208	0.0	5.1	GASBUGGY (NM,USA)
1965 07 15	14 16 08.10	37.197	-74.352	0.0	5.0	CHASE (VA,USA)
1963 10 20	13 00 00.1	24.036	5.039	0		Sahara (Algeria)
1965 02 27	11 30 00.0	24.059	5.031	0		Sahara (Algeria)
*1988 12 04	05 19 52.8	73.45	54.80	0.0	5.9	Novaya Zemlya (USSR)
*1988 08 22	16 19 57.60	66.420	78.580	0.0	5.3	(USSR)
1969 11 30	03 32 59.7	49.924	78.956	0.5	6.0	Kazakh (USSR)
1971 04 25	03 32 59.9	49.769	78.034	0.3	5.9	Kazakh (USSR)
1972 08 16	03 16 59.80	49.765	78.059	0.1	5.0	Kazakh (USSR)
1972 11 02	01 27 00.2	49.927	78.758	0.5	6.2	Kazakh (USSR)

APPENDIX C

Calculation of traveltimes

The calculation scheme used to generate the traveltimes for a given distance for the *iasp91* model was developed by Buland & Chapman (1983)—this paper will be subsequently denoted by BC83. This technique is based on the properties of the delay time τ as a function of slowness p.

For slowness (ray parameter) p, the delay time

$$\tau(p) = T(p) - pX(p), \tag{C1}$$

where $T(p)$ is the traveltime and $X(p)$ is the corresponding range. If we seek the traveltime corresponding to a specified distance x, it is convenient to introduce the theta function

$$\theta(p, x) = \tau(p) + px = T(p) + p[x - X(p)]. \tag{C2}$$

The stationary points of $\theta(p, x)$ as a function of slowness p correspond to geometrical arrivals at the distance x, i.e.

$$\left.\frac{\partial\theta(p, x)}{\partial p}\right|_{p_x} = 0 \qquad \text{when} \qquad x = X(p_x). \tag{C3}$$

This property is exploited by Buland & Chapman, who introduce a novel form of spline representation for the $\tau(p)$ behaviour of a traveltime branch. Consider a tau branch which is sampled at the N slowness values

$$p_0 < p_1 < \cdots < p_{N-1} = p_{\text{end}}; \tag{C4}$$

then a τ-spline approximation which takes care of the square root singularity in the derivatives of $\tau(p)$ at the highest slowness p_{end} is

$$\tau(p) = a_i + b_i(p_{\text{end}} - p) + c_i(p_{\text{end}} - p)^2 + d_i(p_{\text{end}} - p)^{3/2}, \qquad p_i \le p_{i+1}. \tag{C5}$$

The details of the construction of such τ-splines are given in the Appendix to BC83. The range $X(p)$ can be constructed from (C5) by taking the derivative with respect to p:

$$X(p) = -\tau'(p) = b_i + 2c_i(p_{\text{end}} - p) + (3/2)d_i(p_{\text{end}} - p)^{1/2}, \qquad p_i \le p \le p_{i+1}. \tag{C6}$$

The extrema of the theta function, which define the geometrical arrivals at x occur when

$$2c_i(p_{\text{end}} - p) + (3/2)d_i(p_{\text{end}} - p)^{1/2} + (b_i - x) = 0, \tag{C7}$$

which is a quadratic in $(p_{\text{end}} - p)^{1/2}$. Once the geometric slowness p_x has been determined by solving (C7) we can construct the traveltime at x by combining the results from (C5) and (C6):

$$T(x) = \tau(p_x) + p_x X(p_x). \tag{C8}$$

This process may appear quite complex, but has the advantage of yielding traveltime as an explicit function of range. The calculations can be performed very rapidly and are competitive with standard table look-up. However, there is the major advantage that once the $\tau(p)$ distribution has been constructed for a particular phase, exactly the same procedure is to be applied for all phases.

The first stage in the construction of the requisite tau tables is the discretization of the slowness domain and also the establishment of a set of depths between which the tau integrals over the velocity model will be calculated. It is convenient to sample the model at the discrete slowness grid used in the representation of the tau branches. In this discretization certain critical slownesses must be sampled exactly. These are the slownesses just above and below each first-order discontinuity, the slowness at any discontinuity in velocity gradient and local slowness extrema. The discretization between critical point is arranged so that the range for the tau branch is sampled at approximately equal intervals.

The calculation of the $\tau(p)$ distribution along each branch is carried out by summing the analytic results for segments of the model represented as linear slowness gradients BC83 (equation 42). The basic organization of the tau tables for the *iasp91* model is similar to that described for PEMC in BC83. The values for a surface source are calculated for the full range of ray parameters, and also the τ-segments for upgoing waves for each of the discrete depths which are likely to be of interest (down to 760 km). It is convenient to divide the surface tau results into mantle, core and inner core contributions. The full range of upgoing, downgoing and surface reflected phases can then be assembled by suitable addition and subtraction of segments. For example for a source at depth, the $\tau(p)$ for the downgoing S phase can be constructed by subtracting the appropriate upgoing τ values from those for a surface source. The $\tau(p)$ values for *sS*, on the other hand, are to be found by adding the upgoing values to the surface source τ values.

In this way it has been possible to build up appropriate $\tau(p)$ tables for a wide selection of the main seismic phases. Table C1 presents sample outputs from the traveltime routine for a source at 300 km depth and epicentral distances of 50° and 150°. These results show the power of the calculation scheme in handling triplications (e.g. in *PP*, *SS* at 50° and *PKP* at 150°) and also in providing the full range of information for each phase which might be needed for earthquake location work.

APPENDIX D

Introduction of regionalization

The style of the *iasp91* velocity model was chosen to be such as to facilitate the replacement of the crust and upper mantle portion of the model with a structure more representative of a particular region. The simplest way to make such a change is to select one of the upper mantle discontinuities and to replace the velocities above this level.

However, such a substitution has to be undertaken with some care if the entire pattern of teleseismic arrivals is not to be disrupted. As discussed in Appendix C, the technique we have employed for the calculation of traveltimes is based on $\tau(p)$ tabulations. By changing the shallow velocity model, the times in the regional zone can be modified and

Table C1. Phase information at selected distances.

Source depth (km): 300

delta	#	code	time(s)	(min	s)	dT/dD	dT/dh
50.00	1	P	504.25	8	24.25	7.47E+00	-9.20E-02
	2	pP	567.26	9	27.26	7.74E+00	9.00E-02
	3	PcP	579.21	9	39.21	3.70E+00	-1.11E-01
	4	sP	600.95	10	0.95	7.67E+00	2.01E-01
	5	PP	622.56	10	22.56	9.04E+00	-7.84E-02
	6	PP	629.21	10	29.21	1.00E+01	-6.67E-02
	7	ScP	785.39	13	5.39	4.30E+00	-2.10E-01
	8	PcS	816.74	13	36.74	4.31E+00	-1.09E-01
	9	S	911.98	15	11.98	1.38E+01	-1.70E-01
	10	PKiKP	983.93	16	23.93	1.06E+00	-1.15E-01
	11	sS	1024.69	17	4.69	1.42E+01	1.67E-01
	12	pPKiKP	1059.64	17	39.64	1.05E+00	1.15E-01
	13	ScS	1062.98	17	42.98	6.86E+00	-2.04E-01
	14	sPKiKP	1090.15	18	10.15	1.05E+00	2.14E-01
	15	SS	1130.58	18	50.58	1.58E+01	-1.53E-01
	16	SS	1149.73	19	9.73	1.80E+01	-1.30E-01
	17	SKiKP	1166.98	19	26.98	1.11E+00	-2.13E-01
	18	PKKPdf	1847.12	30	47.12	-1.09E+00	-1.15E-01
	19	SKKPdf	2030.13	33	50.13	-1.04E+00	-2.14E-01
	20	PKKSdf	2060.64	34	20.64	-1.04E+00	-1.15E-01
	21	SKKSdf	2243.53	37	23.53	-9.97E-01	-2.14E-01
	22	P'P'df	2350.49	39	10.49	-1.37E+00	-1.15E-01
	23	P'P'bc	2369.77	39	29.77	-2.09E+00	-1.14E-01
	24	P'P'ab	2401.28	40	1.28	-4.29E+00	-1.09E-01
	25	S'S'df	3175.96	52	55.96	-1.11E+00	-2.13E-01
delta	#	code	time(s)	(min	s)	dT/dD	dT/dh
150.00	1	PKPdf	1149.05	19	9.05	1.55E+00	-1.15E-01
	2	PKPbc	1154.67	19	14.67	2.52E+00	-1.13E-01
	3	PKiKP	1155.78	19	15.78	2.07E+00	-1.14E-01
	4	PKPab	1161.44	19	21.44	4.16E+00	-1.09E-01
	5	pPKPdf	1224.48	20	24.48	1.58E+00	1.15E-01
	6	pPKPbc	1229.25	20	29.25	2.62E+00	1.13E-01
	7	pPKiKP	1230.83	20	30.83	2.07E+00	1.14E-01
	8	pPKPab	1233.81	20	33.81	4.09E+00	1.09E-01
	9	sPKPdf	1255.06	20	55.06	1.57E+00	2.13E-01
	10	sPKPbc	1260.03	21	0.03	2.60E+00	2.12E-01
	11	sPKiKP	1261.49	21	1.49	2.07E+00	2.13E-01
	12	sPKPab	1265.08	21	5.08	4.11E+00	2.10E-01
	13	SKPdf	1333.35	22	13.35	1.43E+00	-2.13E-01
	14	PKSdf	1363.91	22	43.91	1.42E+00	-1.15E-01
	15	PP	1372.11	22	52.11	5.73E+00	-1.02E-01
	16	SKSdf	1547.76	25	47.76	1.30E+00	-2.13E-01
	17	pSKSdf	1653.89	27	33.89	1.32E+00	1.15E-01
	18	PKKPdf	1677.93	27	57.93	-1.91E+00	-1.14E-01
	19	sSKSdf	1684.43	28	4.43	1.31E+00	2.13E-01
	20	SKKSac	1751.57	29	11.57	5.52E+00	-2.07E-01
	21	SKKPdf	1864.02	31	4.02	-1.91E+00	-2.13E-01
	22	PKKSdf	1894.65	31	34.65	-1.91E+00	-1.14E-01
	23	SKKSac	2026.13	33	46.13	-3.70E+00	-2.11E-01
	24	SKKSdf	2080.74	34	40.74	-1.91E+00	-2.13E-01
	25	SS	2504.71	41	44.71	1.10E+01	-1.87E-01
	26	S'S'ac	2560.51	42	40.51	7.32E+00	-2.02E-01
	27	S'S'ac	2913.42	48	33.42	-4.49E+00	-2.10E-01
	28	S'S'df	3005.91	50	5.91	-1.92E+00	-2.13E-01

this is equivalent to modifying the $\tau(p)$ values for large slownesses. If the *iasp91* times at teleseismic distances are to be maintained, then the $\tau(p)$ values for the new structure should match those for *iasp91* for all slownesses *less* than the critical slowness for the underside of the discontinuity which marks the base of the section of modified velocity model.

Alternatively, the new portion of the velocity model could be devised to give a specific offset from the $\tau(p)$ behaviour for *iasp91*. This procedure would force an advance or a retardation of the traveltimes to telseismic distances from a particular source region. In this way one could, for example, impose and oceanic crust and uppermost mantle on the 'continental' model *iasp91*.

Such an approach to regionalization is well adapted to describing the behaviour of the traveltimes across a broad zone. In regions of strong lateral heterogeneity, it will probably prove necessary to devise ways in which a 3-D local structure can be graded into a 1-D model at depth. Buland & Chapman (1983) have indicated how the method of traveltime calculation based on the extrema of the theta function, which has been employed to generate the *iasp91* tables, can be extended to laterally varying media.